2010

Characterizing the effects of turbulence on sediment oxygen and sediment nitrate demand using flow-through reactors

Brandon J. Ellefson
Michigan Technological University

Characterizing the Effects of Turbulence on Sediment Oxygen and Sediment Nitrate Demand Using Flow-Through Reactors

By
Brandon J. Ellefson

A THESIS

Submitted in partial fulfillment of the requirements

For the degree of

MASTER OF SCIENCE IN ENVIRONMENTAL ENGINEERING

MICHIGAN TECHNOLOGICAL UNIVERSITY

2010

This thesis, “Characterizing the Effects of Turbulence on Sediment Oxygen and Sediment Nitrate Demand Using Flow-Through Reactors,” is hereby approved in partial fulfillment of the requirements for the degree of MASTER OF SCIENCE IN ENVIRONMENTAL ENGINEERING.

DEPARTMENT

Civil and Environmental Engineering

Signatures:

Thesis Advisor_____
Dr. Martin T. Auer

Department Chair_____

Dr. William M. Bulleit

Date_____

Abstract

Onondaga Lake has received the municipal effluent and industrial waste from the city of Syracuse for more than a century. Historically, 75 metric tons of mercury were discharged to the lake by chlor-alkali facilities. These legacy deposits of mercury now exist primarily in the lake sediments. Under anoxic conditions, methylmercury is produced in the sediments and can be released to the overlying water. Natural sedimentation processes are continuously burying the mercury deeper into the sediments. Eventually, the mercury will be buried to a depth where it no longer has an impact on the overlying water. In the interim, electron acceptor amendment systems can be installed to retard these chemical releases while the lake naturally recovers. Electron acceptor amendment systems are designed to meet the sediment oxygen demand in the sediment and maintain manageable hypolimnion oxygen concentrations. Historically, designs of these systems have been under designed resulting in failure. This stems from a mischaracterization of the sediment oxygen demand. Turbulence at the sediment water interface has been shown to impact sediment oxygen demand. The turbulence introduced by the electron amendment system can thus increase the sediment oxygen demand, resulting in system failure if turbulence is not factored into the design.

Sediment cores were gathered and operated to steady state under several well characterized turbulence conditions. The relationship between sediment oxygen/nitrate demand and turbulence was then quantified and plotted. A maximum demand was exhibited at or above a fluid velocity of 2.0 $mm \cdot s^{-1}$. Below this velocity, demand decreased rapidly with fluid velocity as zero velocity was approached. Similar relationships were displayed by both oxygen and nitrate cores.

Acknowlegements

The knowledge and valuable experiences that I have gained throughout the course of my masters degree are priceless. My success would not have been accomplished had it not been for numerous individuals who helped me in my journey.

I first want to thank my research mates Albert Galicinao and Phillip Depitro. If it was not for their assistance and guidance in the beginning stages of my research, I never would have made it this far.

To Dr. Edwin Cowin and P.J. Rusello for performing the turbulence analysis on our core design and assisting in setting up, maintaining, and running our equipment every step of the way.

The Upstate Freshwater Institute team for helping me every step of the way through my research. I especially want to thank Dr. Effler for giving me a home to perform my research in and for providing me with ample support through my rough times. To Dr. Matthews for working intimately with me in perfecting my experimental design and for spending time teaching and learn with me through my research. I want to thank Mike and Bruce for putting up with our absurd research hours and taking us out on the boat to gather cores on numerous occasions. I would also like to thank the whole UFI laboratory crew (Mary, Melanie, Gina, Mike, Craig, Sarah, Chris, Stephanie, Whitney) for all their hard work, assistance, and moral support.

To Dave Perram for staying in late hours to work with me and help me on a moment's notice on problems he probably shouldn't have to deal with. Thanks for being the world's greatest lab supervisor.

To Rob Fritz and Jesse Nordeng for building our experimental setup and providing us with machine working help throughout the project.

To my research assistants, (Justin, Ken, Kevin) for continuously helping me with my research and helping me manage the numerous experiments that we ran during my time here. I would not have been able to finish without your help.

To the MTU staff for being such wonderful and helpful teachers. There is no other school that could even come close to competing with the positive and personal learning experience that I have attained during my 6 years here. The knowledge that I have gained through my experiences here has prepared me for anything the environmental engineering field has to offer.

To my committee members, Dr. Noel Urban, Dr. Robert Keen, and Dr. Dave Hand for agreeing to be on my committee and helping me through the final stages of my work here.

And finally above all, I would like to thank my amazing advisor Dr. Auer. Thanks for your countless hours of one on one work to train me as a researcher, scientist, and engineer. You never doubted my abilities and you always drove me to perform my very best work. Your training and conditioning has prepared me for anything the world has to offer. You have successfully transformed this college student into a professional engineer. I can't even imagine having a better advisor. Thank you so much for all your help.

Table of Contents

List of Tables

List of Figures

1.0 Introduction

1. 1 Primary Production, Decomposition and Water Quality

The production of aquatic biomass is generally dependent on the availability of a specific limiting nutrient. In most lake ecosystems, phosphorus is the nutrient limiting the production of organic matter (Correll, 1998). Autochthonous production can be decomposed by aquatic organisms in the water column or in the sediments. In eutrophic systems, often times the production of organic matter exceeds the decomposition and, as a result, organic matter will accumulate at the sediment surface.

Phytoplankton and other organic matter that sinks to the lake bottom will be degraded by microorganisms in the sediments (Beutel, 2003). In this redox process, electron acceptors such as oxygen and nitrate are removed from the water, creating a sediment oxygen demand (SOD) and sediment nitrate demand (SND). Most of the redox reactions in soils and aquatic environs are biologically mediated. Under oxic conditions, oxygen is utilized as the electron acceptor and organic carbon serves as the electron donor (Graetzs et. al. 1973). During the summer and winter months, thermal stratification limits mixing and thus prevents replenishment of the hypolimnion with oxygen. If the SOD is too great, hypolimnetic anoxia will result, leading to degradation of water quality through a loss of benthic communities, extirpation of fish species, and a loss of biodiversity (Carpenter et al. 1969). Anoxic conditions can also result in a phenomenon termed internal nutrient loading where phosphorus is released from the lake sediments and can lead to increased phytoplankton and macrophyte growth (Nurnberg 1984). Ultimately, eutrophic conditions will ensue. Other undesirable

substances can be released from lake sediments under anoxic conditions, including ammonia, iron, manganese, sulfide, and methylmercury (Beutel, 2006).

1.2 Approaches to Combating Hypolimnetic Anoxia

The most direct approach to combat hypolimnetic anoxia involves a combination of nutrient management and dredging. Nutrient management seeks to reduce point and nonpoint sources of the limiting nutrient, in this case phosphorus. This prevents over production of organic matter and, over time, aides in reducing oxygen demand. Dredging is used to directly remove legacy deposits of organic matter and their associated SOD.

Where dredging is impractical due to cost or technical feasibility, other methods of combating anoxia may be applied. Among these, the addition of oxygen as air or pure oxygen to facilitate the oxidation of organic matter in the sediments is particularly common. Maintaining oxygen levels above the sediments can prevent nutrient and metal exchange between the water column and the sediments (Beutel 2003, Gemza 1997, Sundby 1986) and promote the health of aquatic species. Nitrate addition also serves to support oxidation of sediments achieving control of chemical releases (Feibicke, 1997; Hansen et al. 2003; Ripl 1976).

1.3 Anoxia and Mercury Cycling

Mercury enters aquatic systems in the elemental (Hg^0; Effler 1996; Ullrich et al. 2001) and ionic (Hg^{2+}) forms (Manohar et al. 2002; Swain et. al. 1992). Deposition from the atmosphere is largely in the form of inorganic mercury (Winfrey and Rudd 1990). “In oxic waters, Hg^{2+} will complex with inorganic ligands (eg. Cl^-, OH^-), bind with dissolved organic carbon (DOC) or sorb to particulate matter” (Effler 1996). In the water column,

but particularly in the sediments, inorganic mercury can be converted to an organo-mercurial neurotoxin (methyl mercuric ion or methylmercury; Dales et al. 1970). This presents a serious risk to human health through bioaccumulation where methylmercury becomes more concentrated in organisms as it moves up the food chain, presenting a higher risk to species higher on the chain (Watras et al. 1998). It is for this reason that methylmercury contamination is intensively studied. A summary of the mercury cycle is displayed in Figure 1.1.

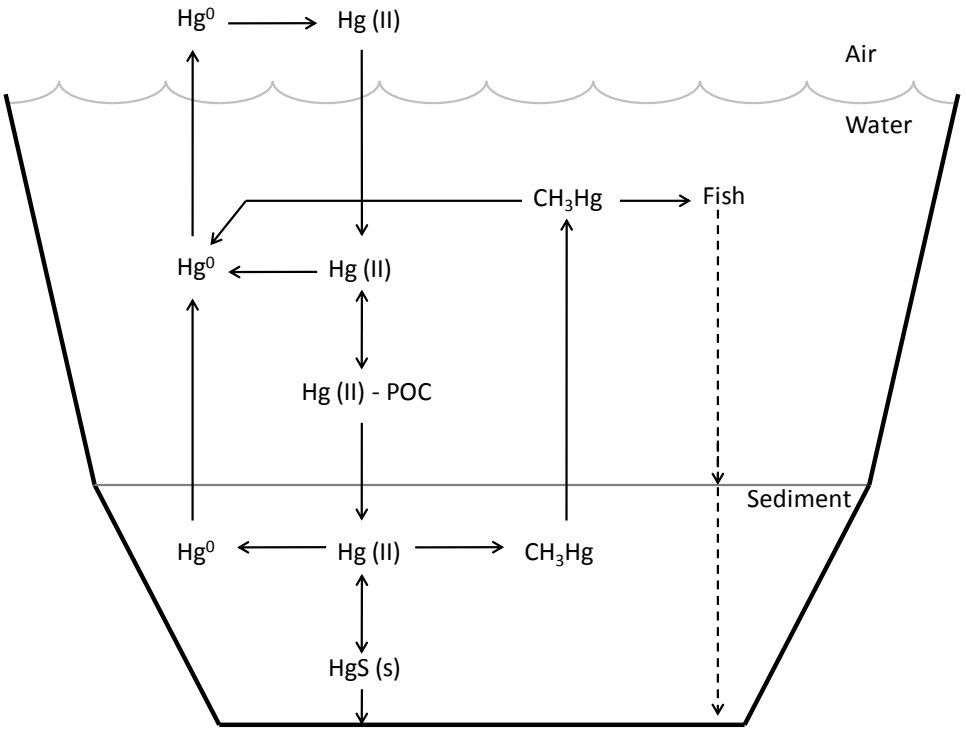

Figure 1.1: The major components of the mercury cycle in an aquatic ecosystem (Driscoll et al. 1994)

Studies have shown that methylation of mercury is generally a microbially mediated process (Jensen and Jernelov 1969; Ullrich et al. 2001). Recent evidence has shown that sulfate-reducing bacteria are mainly responsible for the synthesis of methylated Hg species from elemental mercury (Pak and Bartha 1997; Lambertsson and Nilsson 2006;

Ullrich et al. 2001). The methylated mercury can then diffuse through the sediments into the water column where it is free to bioaccumulate. Under conditions of thermal stratification, methyl mercury can accumulate in the hypolimnion until turnover, after which it will be distributed throughout the system (Parks et. al. 1989).

Prerequisites for mercury methylation include anoxic conditions, the presence of Hg^{2+}, the availability of sulfate (as the electron acceptor), and a labile carbon source (as the electron donor; Lambertsson and Nilsson 2006).

1.4 The Role of Organic Matter in Mercury Methylation

In addition to providing the electron donor required for sulfate reduction, organic matter content influences the location of the process within the sediment. The organic matter accumulating in the sediments is decomposed through oxidation-reduction (redox) reactions and exerts a demand on the electron acceptor resources of the water column. Electron acceptors are utilized in the sequence of their thermodynamic favorability (energy yield), i.e. the ecological redox series or ERS: O_2, NO_3, Mn^{+4}, Fe^{+3} and SO_4^{2} (Matthews and Effler 2008). When these electron acceptors are no longer available, decomposition proceeds through methanogenesis.

Since mercury methylation is primarily associated with sulfate reducing bacteria (Pak and Bartha 1997), the process becomes localized at sediment depths where electron acceptors higher than SO_4^{2-} in the ERS have been depleted (Parks et. al. 1989). Oxygen is depleted nearest the surface, followed by nitrate reduction and, if present in sufficient quantities, manganese and iron. At this point, sulfate reduction takes over as the predominant process, during which mercury is methylated and released to diffuse through the pore water.

The organic matter content of the sediment is a factor that influences the depth of electron acceptor penetration into the sediments (Lambertsson and Nilsson 2006). High organic matter content of the sediments promotes rapid consumption of electron acceptors. Under high rates of consumption, the electron acceptors are consumed before they can diffuse to deeper depths in the sediment. This effectively thins each zone of electron acceptors in the sediments. Low organic matter content results in slower consumption of electron acceptors. This allows for deeper penetration of electron acceptors and forces the methylation process deeper into the sediments, thus aiding in preventing methyl mercury from reaching the water column through diffusion.

1.5 Methylmercury Sinks – The Role of Oxygen and Nitrate

The methylmercury produced in the sulfate reduction layer diffuses through the sediments where it may undergo further transformation. Gagnon et al. (1996) have shown that methylmercury is not able to escape through the oxic layer of the sediments to the overlying water, likely a result of physicochemical adsorption (Reimers and Krenkel 1974) and oxidative demethylation (Lambertsson and Nilsson 2006). Natural clays and organic sediments have been shown to sorb fairly strongly with mercury (Reimers and Krenkel 1974) aiding with burial. Oxidative demethylation is performed by several aerobic and anaerobic microorganisms, but it is predominantly accomplished by aerobic species (Ullrich et. al. 2001). Hines et al. (2000) and Oremland et al. (1995) have shown that oxidative demethylation is most pronounced at the sediment surface, where oxygen and nitrate layers persist. Thus as methylmercury diffuses up from the sulfate reduction layer, it may become absorbed and demethylated, preventing its escape to overlying waters. Thicker oxygen and nitrate layers provide a longer distance over which methylmercury is exposed to sink processes as it diffuses upward. The

oxygen penetration depth (layer thickness) reflects a balance between the carbon degradation rate and the rate of oxygen transport (diffusion and advection) from the hypolimnion into the sediments (Cai and Sayles 1995).

2.0 Focus of Research

2.1 Study Site

Onondaga Lake (Figure 2.1) is an urban system located in Syracuse New York (lat. 43°06'54"N; long 76°14'34"W). It is a hypereutrophic, dimictic lake with a short hydraulic residence time, flushing 2.5 – 5 times annually (Devan and Effler 1984). It possesses a surface area of 11.7 km^2, a mean depth of 12.0 m, a maximum depth of 20.5 m, and a volume of 1.41 x 10^8 m^3 (Wodka et al. 1985). Onondaga Lake is roughly 10 km long and 2 km wide with the long axis being oriented in a north west to south east direction (Effler 1996). Taking into account the lake's morphometry and the fact that topography surrounding the lake is low, wind stress has a significant impact on water motion in the lake (Effler 1996). The lake discharges through a single outlet (1.9km long and 4.5 m deep) into the Seneca River (Effler et. al. 2002). Two major tributaries (Nine Mile Creek and Onondaga Creek) drain the watershed and account for 62% of the annual inflow. The Onondaga County Metropolitan Wastewater Treatment Plant (METRO) discharges its effluent to the lake contributing 19% of the total inflow and the balance comes from smaller tributaries. (Gbondo-Tugbawa and Driscoll 1998).

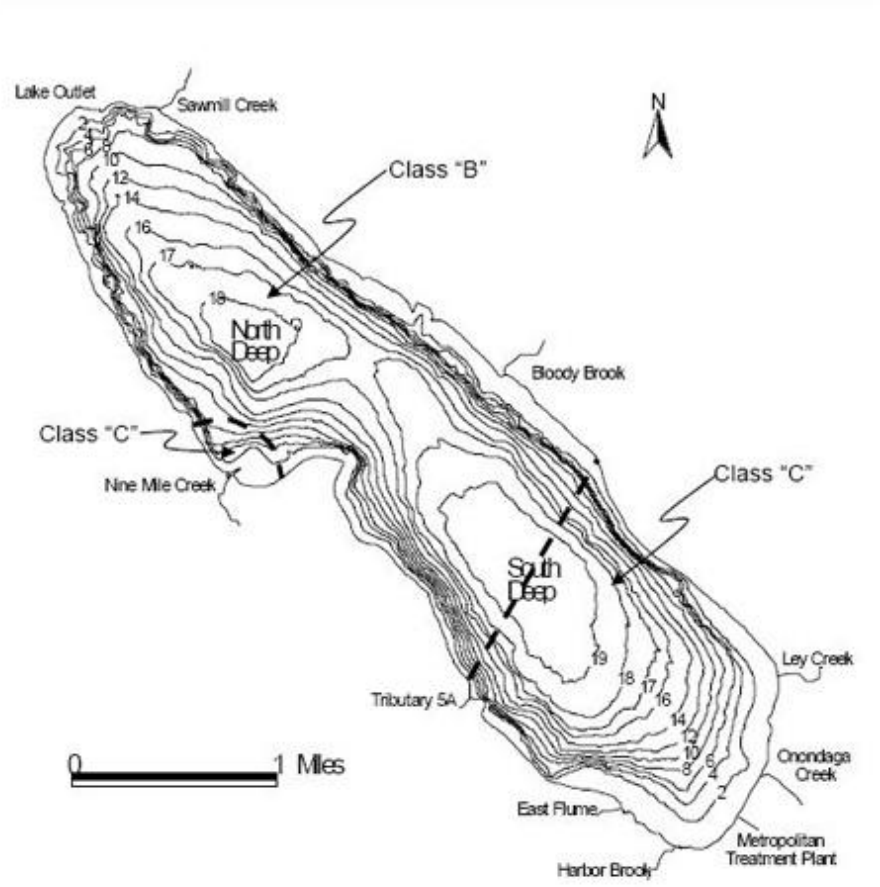

Figure 2.1: Bathymetric map of Onondaga Lake and its tributaries

Onondaga Lake has received the municipal effluent and industrial waste of the region for more than a century (Effler 1996). Treatment at METRO has improved in recent years but effluent continues to be discharged to the lake. Total phosphorus (TP) in Onondaga Lake has decreased from an average of 246.4 $kg \cdot d^{-1}$ between 1900 and 1995 to 100.8 $kg \cdot d^{-1}$ in 2002 (Effler et al. 2002). Raw sewage reaches the lake through tributaries during high runoff events via combined sewer overflows (Effler 1996). As of 2002, the major contributor of TP to Onondaga lake was METRO, providing 77 $kg \cdot d^{-1}$ of the total TP load to the lake (Effler et al. 2002).

Hypolimnetic anoxia occurs in summer as a result of decomposition of organic matter (largely algae) in the sediment (Effler et al. 1988). Oxidation of reduced species accumulating in the hypolimnion has historically depressed water column oxygen concentrations (0 – 4 $mgO_2 \cdot L^{-1}$) at turnover (Effler 1987). Sediment oxygen demand and the attendant duration of anoxia have been in decline (Matthews and Effler 2006). The areal hypolimnetic oxygen deficit (AHOD) averaged 1.08 $g \cdot m^2 \cdot d^{-1}$ from 1997 – 2002, much lower than values reported from previous years, e.g. an average of 2.12 $g \cdot m^2 \cdot d^{-1}$ between 1978 and 1986 (Matthews and Effler 2006). Reductions in AHOD have been attributed to reductions in the delivery of particulate organic matter to the sediment associated with lower phosphorus loading from METRO (Matthews and Effler 2006).

From 1946 to 1986, chlor-alkali processing plants operating on the lake shore discharged mercury to Onondaga Lake. This mercury load, estimated at ~10 $kg \cdot d^{-1}$, resulted in a total of 75,000 kg of mercury being discharged to the lake (Effler 1996). The load was later reduced to 0.5 $kg \cdot day^{-1}$ and direct discharges ceased with closure of the chlor-alkali plant in 1988 (Effler 1996). Legacy deposits of mercury have resulted in elevated concentrations of mercury in the water column (Bloom and Effler 1990), sediment, and fish tissue (Effler 1996). The cycling of methylmercury from the sediment to the water column is linked to hypolimnetic oxygen conditions, as outlined above.

Ongoing lake restoration efforts, e.g. phosphorus removal at METRO (Canale and Effler 1989; Wodka et al. 1983) and upland and littoral sediment remediation at the site of the chlor-alkali process (NYSDEC 2005) promise to yield further improvements in water quality.

2.2 Monitored Natural Recovery with Oxygen and Nitrate Augmentation

Littoral sediments with high levels of mercury contamination will be subjected to a dredge and cap remediation strategy (NYSDEC 2005). The balance of the lake bottom, ~80% of the lake bottom area, will be remediated through monitored natural recovery (MNR). The MNR approach relies on ongoing and naturally reoccurring processes to contain, destroy, or reduce the bioavailability or toxicity of contaminants in the sediments (Zeller and Cushing 2005). The natural processes are aided and monitored over time until remediation goals have been met. The major processes that are responsible for the remediation of sediments are 1) contaminant burial through natural deposition, 2) reduced contaminant mobility through sorption, precipitation and other binding processes, 3) chemical or biological transformations to less toxic forms, and 4) dispersion of particle bound contaminants that leads to contaminant concentration reductions (Zeller and Cushing 2005). In the case of mercury contamination, adsorption and burial are the major processes contributing to monitored natural recovery.

Onondaga Lake has historically had high deposition rates of organic carbon (1.2 – 1.5 $g \cdot m \cdot^{2} d^{-2}$, 1980-86), but rates have declined significantly (0.3 – 0.6 $g \cdot m \cdot^{2} d^{-2}$, 1989-present) mainly due to phosphorus loading reductions at METRO (Upstate Freshwater Institute, unpublished). In MNR, adsorption with attendant burial forces the mercury further and further from the sediment surface, eventually isolating it below the zone of sulfate reduction (methylation). At this point, the mercury is no longer capable of being methylated and will not influence water quality.

In the case of remediation through MNR, a major concern is to minimize the contaminant risk to humans and the environment (Apitz et al. 2005) as the system approaches its

new equilibrium with contaminant and organic carbon loads. It has been demonstrated (Galicinao 2008) that maintenance of oxygen and/or nitrate concentrations above the sediment surface can drastically reduce the internal loading of methyl-mercury. Thus an interim program of oxygen and/or nitrate augmentation can be utilized to resupply the hypolimnion with electron acceptors and inhibit methylmercury flux from the sediment (encourage sorption and demethylation).

2.3 Hypolimnetic Aeration/Oxygenation

It is common practice to use hypolimnetic aeration systems as a restoration tool to replenish the supply of oxygen in lakes, thus preventing hypolimnetic anoxia (McQueen and Lean 1986). Nitrate augmentation has been employed for this purpose in an indirect fashion, through oxidation of organic matter in the sediment (Ripl 1976). In order to properly design an electron acceptor augmentation system, an accurate characterization of sediment oxygen/nitrate demand must be made. There are three accepted methods for estimating that demand: the areal hypolimnetic oxygen deficit (AHOD; Gantzer et al. 2009), steady state measurements made on intact cores (Erickson and Auer 1998; Gelda et al. 1995) and application of the flux gradient method (Jorgensen and Revsbech 1985). Of these AHOD is the most commonly applied in sizing hypolimnetic aeration systems (Beutel 2003; Gantzer et al. 2009). Here, the rate of hypolimnetic oxygen depletion is monitored over the period where the lake remains stratified. Those results are combined with physical parameters such as sediment surface area and hypolimnetic volume to calculate the AHOD (as a demand, $gO_2 \cdot m^{-2} \cdot d^{-1}$). This value provides an estimate of the electron acceptor requirement for MNR with augmentation.

2.4 Induced Oxygen Demand

Surprisingly, this approach has led to underdesign of aeration systems, i.e. the realized AHOD exceeds pre-implementation estimates (Ashley 1983, Soltero et al. 1994, Taggart and McQueen 1982). This phenomenon, termed induced oxygen demand, is thought to be an artifact of the physical-chemical conditions associated with aeration. Induced demand has been observed at several different sites following implementation of hypolimnetic aeration. One such case is a study done on Black Lake in British Columbia (Ashley 1983). The lake was divided in half with a polyethylene curtain and an aerator was used to deliver oxygenated water to the hypolimnion of one half of the lake. The control side of the lake experienced fluxes between 0.03 and 0.09 $mg \cdot L^{-1} \cdot d^{-1}$ while the oxygenated side saw fluxes between 0.39 and 0.78 $mg \cdot L^{-1} \cdot d^{-1}$. This is an increase of about one order of magnitude, suggesting that turbulence and hypolimnion oxygen concentration has an effect on SOD.

In another study on Medical Lake, Washington, a hypolimnetic aerator was installed in an attempt to eliminate phosphorus loading from the sediments (Soltero et al. 1994). After the system was installed, the lake continued to experience anoxia and the AHOD increased to double that of the pre-implementation value. It was concluded that the system was undersized due to errors in accurately quantifying AHOD. The error was thought to be related to turbulence induced by the aerator that was not accounted for in AHOD estimates.

One final study performed to compare different types of oxygen diffusers (Taggart and McQueen 1982). In this study, they predicted AHOD values for their lake and aimed to maintain oxygen levels above the sediments. During this process, efficiencies of the various tested oxygen diffusers were quantified. The results of the study showed that

the AHOD for the lake was inadequately quantified because SOD was out competing the oxygen input by the diffusers. As a result, the lakes remained anoxic.

Induced oxygen demand is thought to occur as a result of elevated electron acceptor levels (Jorgensen and Revsbech 1985; McDonnell and Hall 1969) and enhanced mixing (Beutel 2003; Boynton et al. 1985; Jorgensen and Revsbech, 1985) at the sediment water interface. Oxygen flux at the sediment-water interface is impacted by the oxygen gradient. Higher oxygen concentrations in the hypolimnion provide a stronger driving force for the diffusion of oxygen into the sediments. At low oxygen concentrations, limitation may be experienced (Michaelis-Menten effect), depressing the realized SOD.

It has been demonstrated that turbulence (fluid velocity) at the sediment water interface can also have a significant effect on AHOD/SOD (Arega and Lee 2005; Beutel 2003; Hall et al. 1989; Moore et al. 1997), increasing fluxes by a factor of 2-4 (Ashley 1983; Beutel 2003). Moore et al. (1997) performed a study to understand the factors that caused induced oxygen demand after implementing oxygen diffusion systems in lakes. Experiments were performed with a batch reactor chamber where water was cycled through the chamber. Water exited the reactor at the top and entered it again immediately above and parallel to the sediment surface. Fluid velocity in the core was assumed to be the pumping rate. Oxygen depletion was measured over time and fluid pumping velocity was plotted against oxygen concentration. This provided an understanding that fluid velocity does influence the SOD. Beutel (2003; 2006) performed reactor experiments were turbulence was introduced through a water inlet jet that was placed near the sediment surface. Fluxes were measured for various lakes using high, medium, and low levels of mixing, thus demonstrating the impacts that fluid velocity has on SOD. Arega and Lee (2005) went further by installing two jets into the

top of a reactor to create circulating flow. Fluid velocity was quantified in the core and plotted against SOD for three different sediment types. SOD was calculated in the core using a mass balance, oxygen microprofiles, and a batch experiment setup. Results between the methods could then be compared. The same conclusion was made that turbulence has an impact on SOD.

Fluid velocity affects SOD by altering the thickness of a thin layer of water that exists immediately above the sediment surface and exhibits laminar flow conditions. This layer is termed the diffusive boundary layer (DBL). Viscous forces between the sediment surface and the water slows down fluid flow, creating a thin zone of laminar flow (DBL; Jorgensen and Marais 1990). Fluid velocity at the sediment surface is essentially zero due to these viscous forces. Fluid velocity will increase logarithmically as distance from the sediment surface increases. At some distance from the sediment surface, flow will transition from being dominated by laminar flow (molecular diffusion) to being controlled by turbulent flow (eddy diffusion). The vertical transport of electron acceptors by eddy diffusion is strongly reduced at this transition from turbulent to laminar flow (Gundersen and Jorgensen 1990). Within the DBL (the region of laminar flow) transport is controlled by molecular diffusion (Gundersen and Jorgensen, 1990), a process which resolves concentration gradients much more slowly than eddy diffusion. Under conditions of high turbulence, the DBL is at a minimum thickness, diffusion is at a maximum, and the realized SOD approaches the value (SOD_{max}) dictated by the biogeochemical processes within the sediment. A reduction in turbulence leads to an increase in the thickness of the DBL, reducing diffusive transport and depressing the realized SOD. High turbulence disturbs the DBL and makes it thinner. This results in elevated SOD values due to the minimized distance over which molecular diffusion must occur. Fluid velocity at the sediment surface will always be zero due to viscous forces, but under high enough

turbulence, the DBL will be thinned to a negligible thickness and yield the maximum SOD (SOD_{max}).

The DBL can be visually observed by taking oxygen microprofiles in the sediment of a core. In the bulk liquid, water is mixed thoroughly by turbulent diffusion. Oxygen concentrations will be moderately stable throughout this zone. As the sediments are approached, there will be a transition between turbulent and laminar flow. This is the beginning of the DBL. Oxygen, concentrations are limited by molecular diffusion in this zone and as a result, concentration will decrease linearly throughout the DBL. Once in the sediment, biological consumption and diffusion both reduce oxygen concentrations. Additionally, as oxygen concentrations approach zero, organisms remove oxygen from the water less efficiently. These factors all compound to result in a non linear decrease in oxygen until its ultimate depletion at some depth (Figure 2.2).

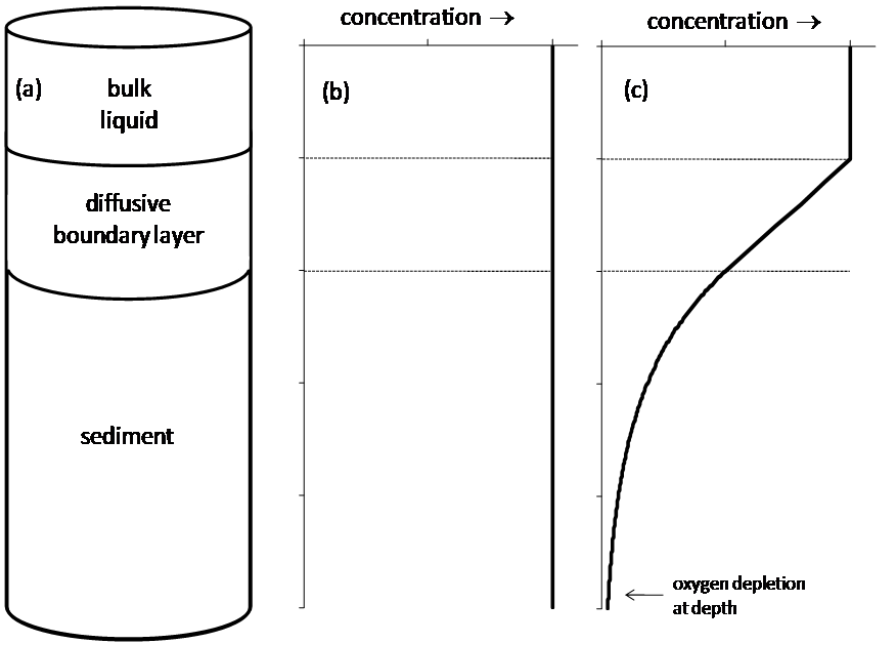

Figure 2.2: Oxygen microprofile of sediments displaying the depletion of oxygen as depth into the diffusive boundary layer and sediments increases.

Implementation of electron acceptor augmentation has the potential to influence both the oxygen/nitrate concentration and the turbulence (DBL thickness) of the system. Thus, the induced electron acceptor demand effect must be taken into consideration in the design of augmentation systems. This is especially true in lake restoration efforts where cost may be critical and the electron acceptor supply rate must efficiently balance the rate of utilization (McDonnell and Hall 1969).

3.0 Objectives, Approach and Experimental Design

The objective of this research was to quantify the potential for induced demand associated with a program of electron acceptor augmentation (with nitrate and/or oxygen) in Onondaga Lake. To that end, a relationship was developed between sediment nitrate and sediment oxygen demand and fluid velocity at the sediment-water interface. That relationship defines threshold velocities for the manifestation of induced demand and facilitates comparison to ambient and post-implementation velocities.

The approach was to utilize flow-through reactors containing intact sediment cores, operated at steady-state conditions, to measure electron acceptor flux (SND/SOD) over a range of fluid velocities. The sediment reactors were designed in collaboration with the Joseph H. DeFrees *Hydraulics Laboratory* at Cornell University, establishing and quantifying reactor turbulence in a manner making it directly comparable to measurements of ambient hypolimnetic turbulence (Cowen and Rusello 2008).

Measurements were made over a range of turbulence levels, with replicate determinations performed at selected velocities. Measurements were often made in a serial fashion, i.e. once a flux was determined for a specified fluid velocity, the pump was adjusted to yield a new velocity and another trial initiated. Fluxes derived in this manner were normalized to facilitate comparison and plotted against the sediment-water interface velocity to develop the desired relationship between turbulence and SOD/SND.

Sediment microprofiles were also collected under various turbulence conditions to calculate SOD and provide a comparison with the steady state core experiment results. Profiles were collected at no less than 5 turbulence conditions under 3 separate bulk liquid concentrations. The relationship between flux and pumping RPM was developed.

4.0 Methods

4.1 Core Collection

Sediment cores were collected on 4 dates over the interval 6/12/08 - 4/26/09, supporting 14 measurements of sediment oxygen demand and 12 measurements of sediment nitrate demand. Cores were collected from the South Deep station (depth, 19m), a site considered representative of sediment conditions in the depositional basins of Onondaga Lake (Effler 1996). Sediments originally collected using a box corer (Model 1260, Ocean Instruments, Inc., San Diego, CA) were sub-sampled using 15.24 cm (6-inch) diameter polycarbonate reactor housings and capped with friction-fit tops and bottoms. The sealed cores were placed on ice and transported to the laboratory. Following collection, cores were stored in the dark at 4°C to slow degradation of the organic matter contributing to SND and SOD. Additionally, the conduct of the experiment itself leads to microbial consumption of organic carbon (Sundby 1986). Where values for SND_{max} and SOD_{max} declined significantly due to length or storage or utilization in measurements, the core was discarded. Laboratory tests demontrated that cores had a 'shelf life' of about 3 months after measurements began, i.e. the associated SOD or SND was unchanged. Results gathered after this sharp decline in flux was observed were discarded.

4.2 Sediment Reactors

Reactors were specifically designed to support the quantification of chemical flux at the sediment-water interface by,

- housing an intact sediment core
- providing an inlet for addition of feed stock
- permitting establishment of specified turbulence levels
- maintaining isotropic and completely mixed conditions; and
- providing an outlet for sample collection.

A major challenge to the design of this reactor is to insure that turbulent flux dominates within the chamber (i.e. mean advective flux is eliminated). Mass transport in the hypolimnion of lakes and attendant chemical renewal at the sediment-water interface occurs primarily through vertical turbulent mixing. Horizontal advective flux in the hypolimnion (spatial scale of 100s of meters) does not serve to renew conditions at the interface, but rather moves water of a relatively constant chemical composition over the bed. In chambers (spatial scale of centimeters), however, horizontal advective transport quickly moves water to the boundary (chamber wall), setting up a circulation pattern that provides chemical renewal at the sediment-water interface. Thus it is the goal of chamber design to establish isotropic conditions, i.e. no net flow. To meet this challenge, a novel chamber was developed based on proven isotropic turbulence generation techniques (Rusello and Cowen 2010). The chamber design minimizes advective horizontal transport by utilizing an array of jets arranged symmetrically on the chamber top and oriented with the jet axes perpendicular to the sediment bed. The jets are driven by peristaltic pumps which randomly change direction, generating nearly isotropic turbulence that is horizontally homogenous with very low mean flows. Pumps were also programmed to operate on three minute cycles to avoid water stagnation. The pumps would pump randomly for two minutes and then all pump in one direction for one minute to flush the tubes.

The second challenge is to quantitatively characterize turbulence within the chamber. Particle image velocimetry (PIV) was used for this purpose, characterizing chamber turbulence under various forcing conditions (Figure 4.1; Cowen and Rusello 2008 Unpublished). Vertical turbulent intensity, calculated as the root mean square difference between the instantaneous and mean velocities, was selected as the metric representing turbulence in the chamber. The turbulent intensity is a common turbulence statistic and provides a measure of the strength of the turbulence readily comparable to field measurements. With appropriate assumptions it can also be used for comparison to other systems where turbulence statistics are not reported. The third challenge is to scale chamber turbulence to that of the ambient environment. Vertical turbulent intensity, the metric adopted for laboratory chambers, is readily measured in the field and its use in characterizing turbulence in the ambient environment facilitates direct comparison of conditions. Measurements in the bottom boundary layer of Onondaga Lake (Rusello and Cowen 2010) showed classic turbulent boundary layer conditions, although with weaker mean flows than expected. Because of the slow mean flows, measurement noise dominates the horizontal turbulence statistics, leaving the vertical turbulence measurements (which have significantly lower measurement noise) as the most reliable estimates of *in-situ* turbulence conditions. Turbulent intensities and turbulent dissipation rates in the chamber were compared to estimates from the field measurements with good agreement at a representative turbulent intensity of 1-2 mm/s. Chamber turbulence conditions were calibrated to the pump speed in RPM, yielding a vertical turbulent intensity appropriate for modeling scalar flux at both current *in-situ* conditions and with enhanced turbulence as may be imparted through electron acceptor augmentation.

Fundamental to the operation of the reactors is the ability to adjust and quantify turbulence at the sediment-water interface while maintaining isotropic mixing conditions. The reactors were sealed to minimize oxygen penetration and operated under a zero head space condition. The reactor top was outfitted with six turbulence jets that were flush with the reactor/water interface. Tygon tubes were run from these jets through 3 peristaltic pumps (Masterflex L/S Computerized Drive; Masterflex Easy Load II Model #77202-50) providing a means of mixing by recirculation.

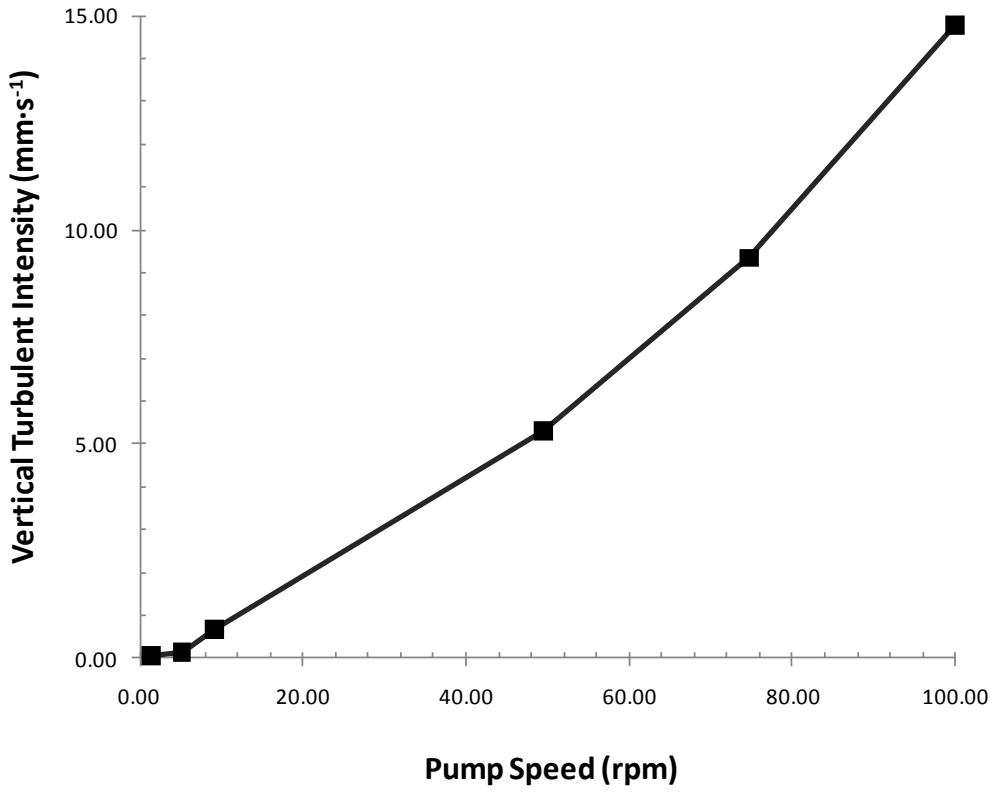

Figure 4.1: The relationship between circulating pump speed (RPM) and vertical turbulent intensity ($mm \cdot s^{-1}$) at the sediment water interface.

The turbulent intensity at the sediment surface was determined by averaging vector diagrams of the fluid flow in the zone between 10 and 20 mm above the sediment surface. This region was selected because it showed essentially constant values for

turbulence intensity throughout the zone. Additional details of the hydrodynamics of this system and its ability to provide variable-turbulence and isotropic mixing are presented by Rusello and Cowen (2010).

Velocities employed here (0-5.3 mm/s, pump speeds of 0-50 RPM) reflects the range of ambient vertical fluid velocities observed near the sediment-water interface of Onondaga Lake. The maximum velocity represents a minimum DBL thickness and thus an appropriate condition for determination of SOD and SND_{max}. Above this maximum velocity, sediment resuspension occurs.

The degree to which induced electron acceptor demand is manifested depends on two factors: turbulence and the electron acceptor concentration in the bulk liquid (Beutel 2003; Jorgensen and Revsbech, 1985). Here, turbulence must be isolated as the sole variable. Concentration effects were isolated by attempting to maintain a single steady state level of oxygen or nitrate in the reactor for all incubations. Target concentrations were selected to match those proposed for control of MeHg flux through electron acceptor amendment (Galicinao 2008).

Oxygen and nitrate levels were maintained by augmenting a feed stock of artificial lake water (ALW) with nitrate and various gases. The ALW mimics the ionic composition of Onondaga Lake and includes a variety of chemical species including Na_2SO_4, NaCl, KCl, KOH, $CaCl_2$, NaF, and $MgCl_2$ (Table A.1). This provides the sediment organisms with a majority of the necessary nutrients that they require to survive. It is assumed that the sediments provide the remainder of the micronutrients that are required for the organisms to function. Feed stock inflow was controlled using rotameters and a gravity feed initially, while peristaltic pumps were utilized later in the experiment due to their ability to maintain better control over the flow rate. Nitrate levels in the SND reactor were

maintained by amending the ALW with KNO_3. The influent nitrate concentration was maintained at a constant value to allow steady state to develop. Depending on the SOD in the core, this constant influent concentration existed in a range between approximately 3.5 and 7.5 $mgN \cdot L^{-1}$ with the goal of achieving a steady state nitrate concentration at 2 $mgNO_3\text{-}N \cdot L^{-1}$ in the effluent. Influent flow rate adjustments were made to fine tune the effluent concentration and achieve a stable concentration closer to 2 $mgNO_3\text{-}N \cdot L^{-1}$. The SND reactor feed stock bottle was continuously bubbled with nitrogen gas to purge oxygen from the system. Influent oxygen concentrations were established by introducing a mixture of air and nitrogen gas (Mix-1000 Digital Gas Mixer/Blender). The same procedure was followed for the oxygen reactor. Influent oxygen concentrations were kept stable at a constant value in the range of 8 and 11.2 $mgO_2 \cdot L^{-1}$ depending on the SOD. Flow rate adjustments were used to fine tune the effluent oxygen concentration and achieve a concentration of 2 $mgO_2 \cdot L^{-1}$.

One factor that needed to be taken into consideration in this experimental setup was the turbulence induced in the reactor by the influent pump. This turbulence was not factored into the fluid velocity measurements made on the core using particle velocimetry. To minimize the impact that this flow rate had on SOD and SND, the influent port was placed approximately 1 inch from the top of the sediment core, and aligned horizontally, as to minimize disturbance on vertical fluid velocity. Additionally, influent flow rates were kept low (between 0.25 and 2.5 $ml \cdot min^{-1}$) to minimize the amount of turbulence added to the core. With these measures taken, the affect that this flow rate would have on the reactor's overall turbulence was assumed negligible.

Another factor that needed to be considered was core acclimation time. Initially after cores were set up, sediment biota were not accustomed to surviving in new conditions at

8 °C. The organisms require time to adjust their metabolic functions to suit the new conditions. As a result, cores were maintained and effluent flux rates were monitored until flux stabilization occurred. After stabilization occurred, flux measurements resumed. Acclimation time generally took on the order of about a week.

Two reactors (one SND and one SOD) were operated simultaneously. Incubations were performed in a constant temperature room (8°C) mimicking ambient hypolimnetic conditions. Cores stored at 4 °C were allowed to acclimate to the 8°C temperature used during measurement to reflect ambient conditions. Effluent concentrations were monitored for several days after placing the core at 8°C to ensure flux stability. Flux measurements were initiated once system stabilization was achieved. The oxygen content of the feed stock was monitored daily (HACH HQ 40d LDO probe). Effluent oxygen concentrations were measured continuously using an inline Unisense oxygen microsensor (100µm tip diameter) with computer data archiving. In order to avoid disturbing the system, the probe was calibrated at the beginning and end of each incubation. The nitrate content of the feed stock was monitored daily with a specific-ion electrode (Orion Thermo Scientific Nitrate Sensor 9700B NWP). Effluent (15-25 mL samples) was collected four times daily and nitrate concentrations were measured using the specific-ion electrode. The electrode was calibrated daily. The sediment reactor system is described schematically in Figure 4.2 below.

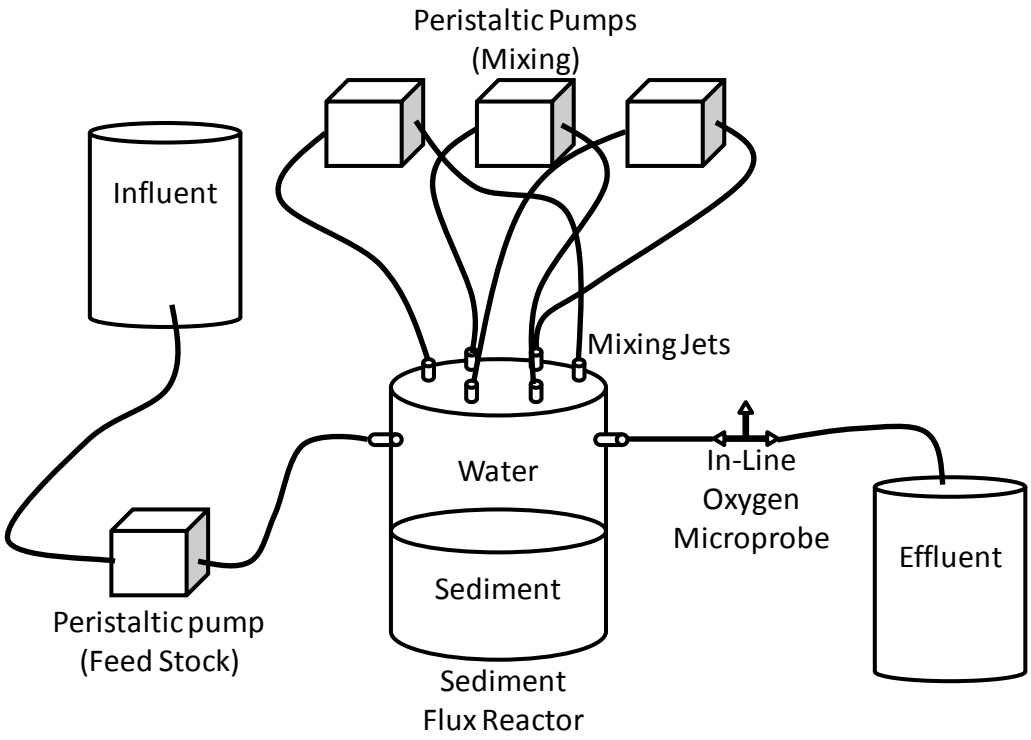

Figure 4.2: Experimental set up for turbulence induced SOD/SND experiment

4.3 Flux Calculation

The sediment reactors were run to steady state and the effluent electron acceptor concentration noted. The flux (SND, SOD) is then calculated using a mass balance:

$$\frac{dC}{dt}V = QC_{in} - QC - JA \qquad [1]$$

where:

C_{in} =	influent oxygen or nitrate concentration	$g \cdot L^{-1}$
Q =	flow rate	$L \cdot day^{-1}$
J =	oxygen or nitrate flux	$g \cdot m^{-2} \cdot day^{-1}$
C =	effluent oxygen or nitrate concentration	$g \cdot L^{-1}$
V =	liquid volume in the sediment reactor	L
A =	Area of the sediment surface	m^2

At steady state, the change in concentration (dC/dt) is zero, and Equation 1 becomes:

$$0 = QC_{in} - QC - JA \quad [2]$$

Rearranging Equation 2, one can solve for the oxygen or nitrate flux:

$$J = \frac{Q(C_{in} - C)}{A} \quad [3]$$

The values for Q, C_{in}, C, and A are all measured during the experiment operation. The fluxes generated by this calculation were obtained using sediment cores collected at various times of the year and thus reflecting a range of sedimentation fluxes (Soltero et al. 1994) and carbon content and lability. These differences manifest themselves through a variation in the value of SOD_{max} and SND_{max}. Thus, fluxes determined for a particular core were normalized against their respective SOD_{max} and SND_{max} value before being added to the pool of data used to define the demand/velocity relationship. This normalization was performed by dividing each of the calculated flux values for a core by that cores respective maximum flux value. Values were then plotted against fluid velocity in the core.

4.4 Sediment Microprofile Determination of SOD

Oxygen microprofiles can also be used to determine SOD. SOD can be calculated with microprofiles using Fick's law of diffusion (Jorgensn and Revsbech 1985).

$$J = D \cdot \frac{dc}{dz} \quad [4]$$

Where:

dc =	Change in concentration	$g \cdot L^{-1}$
dz =	Change in depth	m
D=	Diffusion coefficient	$m^2 \cdot d^{-1}$
J =	Oxygen flux (SOD)	$g \cdot m^{-2} \cdot day^{-1}$

The change in concentration over the change in depth (dc/dz) is found by taking the slope of the oxygen depletion line in the oxygen microprofile. The diffusion coefficient (D) was calculated for oxygen by performing a bromide tracer experiment. Cores were stored with 100 ml of 100 $mg \cdot L^{-1}$ Br^- stock solution for a pre determined set of time intervals. Cores were then harvested by slicing them in 0.5 cm slices. The liquid was extracted from the slices using a centrifuge and Br^- concentrations were determined in the extracted pore water using an ion chromatograph. Details covering the full procedure of this experiment are included in Appendix B. D was calculated to be $3.50*10^{-5}$ $cm^2 \cdot s^{-1}$ using these methods. This coefficient compares favorably to a value determined with a diffusion coefficient calculator developed by the Environmental Protection Agency ($1.31*10^{-5}$ $cm^2 \cdot s^{-1}$). Determinations of flux using microprofiles were all calculated using the experimentally determined diffusion coefficient ($3.50*10^{-5}$ $cm^2 \cdot s^{-1}$).

To compliment the steady state reactor experiment, a microprofile experiment was performed to demonstrate the effects of turbulence on SOD. The original polycarbonate cores were not designed to allow for microprofiling to be performed during operation. As a result, 4'' Teflon sediment reactors were collected via methods described in section 4.1 and designed to meet these needs. These reactors were also designed to meet the same qualifications as those outlined above (section 4.2).

The experimental design and set up is the same as outlined in figure 4.2. The Teflon reactor was outfitted with a 3'' diameter hole in the lid to allow for profiles to be taken through the lid. While in operation, the hole was plugged with a rubber stopper to create a flow through reactor. The reactor was allowed to acclimate for a week under high turbulence conditions that did not disrupt the sediment surface. After acclimation, profiling was performed. Steady state conditions were checked by taking replicate

profiles out of the core over several days and ensuring that sediment conditions were unchanging.

A Unisense microprofiling system was set up to gather sediment profiles. A Unisense picoammeter (PA 2000) was utilized to collect profile data and record it to a computer. A Unisense laboratory stand and micromanipulator (VT-80) were utilized to perform computer controlled microprofiling. A Unisense oxygen microprobe (50µm) was attached to the picoammeter and utilized to take profiles from the core.

The experiment was started by running the sediment reactor to a pre determined steady state bulk liquid concentration. Isotropic mixing was maintained throughout the experiment. Once at steady state, in order to maintain isotropic mixing conditions for profiling, the reactor had to be transformed into a batch reactor by crimping off the influent and effluent ports. This allowed for the removal of the rubber stopper from the reactor lid without draining the water over the sediment.

With the reactor lid removed and mixing conditions preserved, the Unisense oxygen microprobe was attached to the micromanipulator stage and profiles were taken in the core. Profiles began ~3 mm above the sediments and measured down to ~3 mm into the sediments in order to capture the DBL and the depletion of oxygen through the sediments. All profiles gathered were taken approximately 5 cm from the core's center and circled the center of the core. The same location was never profiled twice to prevent taking profiles out of a punctured hole in the sediments. Profiles were gathered with a resolution of 50 µm of depth and repeated until matching profiles resulted. With the sediment conditions characterized through profiles, the turbulent intensity in the core was changed to a new setting, and provided time for the sediments to reach a new steady state. Sediment profiles were gathered for steady state sediment conditions at a

minimum of 5 different turbulence conditions. The experiment was the performed on 3 different bulk liquid concentrations, to quantify the affect that bulk liquid concentration has on SOD.

When performing a microprofile, a zero point needs to be determined where the tip of the profiling needle comes into contact with the sediment surface. Due to our reactors being made of Teflon, determining this point was made more difficult. To determine the zero point, a laser pointer was shined through the open lid of the reactor while lowering the profile needle. The light beam allowed us to see fairly closely when the needle tip contacted the sediments. This method did however result in slight variations in where the zero point was for each profile. As a result, replicate profiles taken out of a core were sometimes offset from one another by several hundred micrometers.

5.0 RESULTS AND DISCUSSION

5.1 Reactor Operation and Performance

The reactor presented in Figure 4.2 was operated over a range of turbulence levels (fluid velocities; 4.1) established by adjusting the speed (RPM) of the mixing pumps. SND and SOD were determined at each turbulence level. Measurements were made at steady state, i.e. when the rate of chemical transfer at the sediment-water interface was in equilibrium with the sediment electron acceptor demand for a particular turbulence condition. Each incubation was run for a period of several days to ensure that steady state was achieved. Depending on antecedent conditions, (flow rate, turbulence, initial bulk liquid concentration) the time to steady state varied by days to over a week. Another factor that influence this time to steady state was the bacterial populations in the sediments. These populations of organisms require time to acclimate to new conditions and build up their populations. The fastest experimental trial performed lasted 5 days, while most took over a week. It is assumed that the bacteria were provided enough time to reach equilibrium based on prolonged measurements of stable oxygen and nitrate concentrations in the effluent of the reactors. The approach to steady state for representative nitrate and oxygen chambers is illustrated in Figure 5.1.

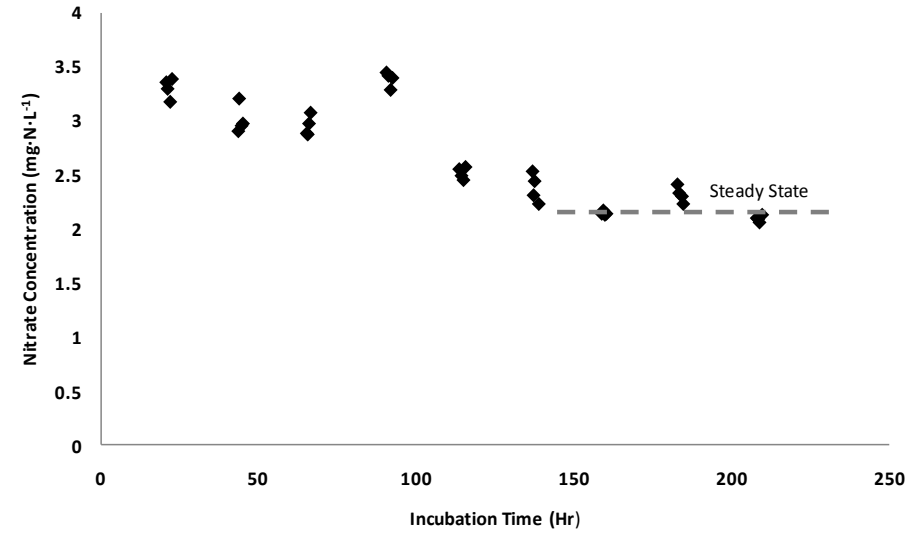

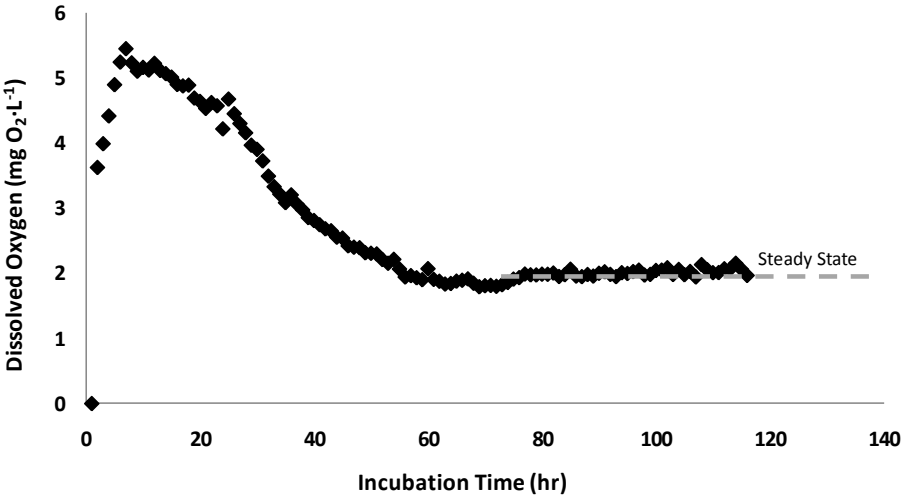

Figure 5.1: Sample appraoch to steady state data for (a) oxygen and (b) nitrate incubations. Oxygen measurements are made continuously (in-line microelectrode), while nitrate measurements are made at discrete intervals (probe).

5.2 Determination of SND and SOD as Functions of Turbulence

Once at steady state, data were collected over a period of 2-4 days to support determination of SND and SOD. The incubation proceeded with effluent measurements of nitrate or oxygen made at regular intervals and an average steady state effluent

concentration calculated. The average concentration was then applied to the mass balance calculation (Equation 3 above) to yield the SND or SOD for a particular experimental condition.

The maximum SND and SOD of a particular core may vary with time of collection due to changes in the amount and nature of the organic matter in the surficial sediment. For this reason, measurements of SND and SOD conducted at different times were normalized to the maximum SND and SOD for that particular core. Here, values of SND_{max} and SOD_{max} were determined for each collection by operating the mixing system at the maximum pump setting (50 RPM). Subsequent fluxes for that collection (measurements made over a range of turbulences) were then normalized to that value for SND_{max} and SOD_{max}.

5.3.1 Sediment Oxygen Demand

A total of 20 incubations were performed, with 15 incubations meeting the criteria of being representative of ambient lake conditions (detailed in section 5.0). All of the incubations that were included in the analysis resulted in an average steady state oxygen concentration of 2.96 ± 1.86 $mgO_2 \cdot L^{-1}$. The incubations yielded values of SOD_{max} ranging from 1.01 to 1.25 $gO_2 \cdot m^{-2} \cdot day^{-1}$ with an average of 1.09 ±.11. $gO_2 \cdot m^{-2} \cdot day^{-1}$ (Table A.2.). Due to the clustering of the data, the median value of 1.05 $gO_2 \cdot m^{-2} \cdot day^{-1}$ may be considered a more accurate representation of the results. The average and median values for SOD_{max} compare favorably with contemporary areal hypolimnetic oxygen demand values determined by the Upstate Freshwater Institute (1.02 $gO_2 \cdot m^{-2} \cdot day^{-1}$; UFI, unpublished data 2009). The contemporary average value is also ~35%

lower than that reported for the early 1990's (1.68 ± 0.56 $gO_2 \cdot m^{-2} \cdot day^{-1}$; Gelda et al. 1995).

SOD values over the range of turbulences were normalized to the SOD_{max} value for their particular collection and plotted against vertical fluid velocity (Figure 5.2). The line of best fit was determined by performing a root mean square error (RMSE) analysis (Table 1). The standard error from the line of best fit was 0.17. A single point (open circle in Figure 5.2) clearly departed significantly from the line of best fit for the data. This point has an error 2.5 times greater than the standard error and as a result, was considered an outlier and excluded from the following analyses. The relationship between turbulence (velocity, mm/s) and SOD is well described by a rectangular hyperbola (Equation 5),

$$SOD_{\nu} = \alpha \cdot SOD_{\max} \cdot \frac{\nu}{\beta + \nu} \qquad [5]$$

where SOD is the sediment oxygen demand at velocity (ν) and where SOD_{max}, as applied in equation 5, is 1.0 (i.e. the normalized maximum SOD). The best fit curve was determined by performing a root mean square error analysis (Table 1). Errors were minimized and the optimum fitting parameters that resulted were α = 1.05 and β = 0.2 (both dimensionless). This yielded a root mean square error of 0.013 $gO_2 \cdot m^{-2} \cdot day^{-1}$ for the model fit to observed average fluxes. The 'elbow' in the curve (Figure 5.2), where a departure from SOD_{max} is first noted, occurs at a velocity of ~1.5 $mm \cdot s^{-1}$. Below this elbow, SOD decreases in a near linear fashion with decreasing fluid velocities

Data compiled in Figure 5.2 was then averaged and plotted with error bars (Figure 5.3) to better see the SOD/turbulence relationship.

Table 1: Root mean square error analysis of normalized oxygen flux data to minimize the error in plotting the best fit for the flux data.

#	Velocity ($mm \cdot s^{-1}$)	Modeled Value	Actual Value	Error	Error ^{2}
1	0.04	0.175	0.47	0.2950	0.08703
2	0.2	0.525	0.74	0.2150	0.04623
3	0.2	0.525	0.79	0.2650	0.07023
4	0.68	0.811	0.64	-0.1714	0.02937
5	0.68	0.811	0.72	-0.0914	0.00835
6	0.68	0.811	0.61	-0.2014	0.04055
7	1.5	0.926	0.94	0.0135	0.00018
8	2.35	0.968	1.00	0.0324	0.00105
9	2.35	0.968	0.95	-0.0176	0.00031
10	2.35	0.968	1.00	0.0324	0.00105
11	2.35	0.968	1.36	0.3924	0.15394
12	5.31	1.012	1.00	-0.0119	0.00014
13	5.31	1.012	1.00	-0.0119	0.00014
14	5.31	1.012	1.00	-0.0119	0.00014
				Standard Error	0.1770165
				Mean	0.0313
				Root Mean	0.1770
				RMSE	**0.0126**

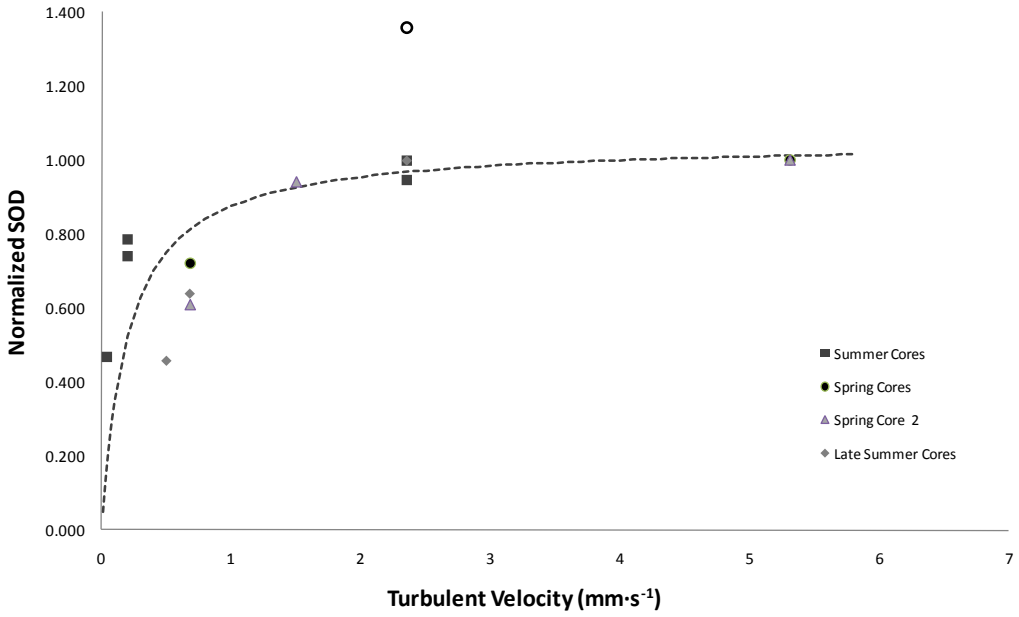

Figure 5.2: Normalized SOD values from four separate sediment cores plotted against the vertical fluid velocity at the sediment water interface

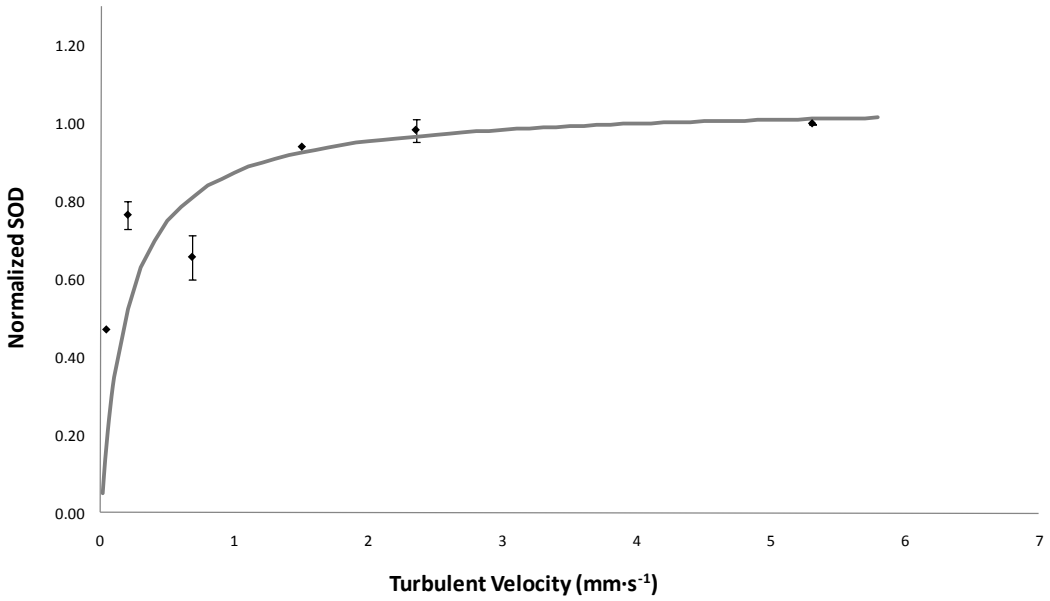

Figure 5.3: Averaged normal SOD values from Figure 5.2 plotted with error bars

5.3.2 Sediment Nitrate Demand

A total of 15 incubations were performed yielding an average steady state nitrogen concentration in the bulk liquid of 2.12 ± 0.76 $gN \cdot m^{-2} \cdot day^{-1}$. This is very close to the target of 2.0 $mgN \cdot L^{-1}$. Results for SND_{max} ranged from 0.079 - 0.258 $gN \cdot m^{2} \cdot day^{-1}$ with an average of 0.17 ± 0.07 $gN \cdot m^{-2} \cdot day^{-1}$. These values are fairly similar to rates of areal hypolimnetic nitrate demand determined by the Upstate Freshwater Institute (0.07 - 0.09 $gN \cdot m^{-2} \cdot day^{-1}$; UFI, unpublished data for 2008 and 2009) and are significantly less than those determined in years past (Upstate Freshwater Institute, unpublished).

Resulting flux values were normalized against their respective maximum values (Figure 5.4) and a RMSE analysis was performed to find the line of best fit (Table 2). The standard error calculated from the line of best fit to the data was 0.074. A single point (open circle in Figure 5.4) clearly departed from the line of best fit. It had an error two

times higher than the standard error and as a result, was excluded from the analysis. Equation 5 was utilized to develop the SND and turbulence relationship.

$$SND_{\nu} = \alpha \cdot SND_{\max} \cdot \frac{\nu}{\beta + \nu} \quad [6]$$

A root mean square analysis (Table 2) was done to minimize error in the line of best fit and resulted in the fitting parameters (Equation 6) of α = 1.02 and β = 0.1 (both dimensionless) and yielded a root mean square error of 0.006 $gN \cdot m^{-2} \cdot day^{-1}$ for the model fit to observed average fluxes. The elbow in the SND-velocity nitrate curve occurs at ~1.0 $mm \cdot s^{-1}$, which is fairly close to that observed for SOD.

Table 2: The root mean square error analysis to minimize the error in the curve of best fit for the nitrate flux data.

#	Velocity ($mm \cdot s^{-1}$)	Modeled Curve	Actual Value	Error	Error ^{2}
1	0.04	0.290	0.29	0.0000	0.00000
2	0.04	0.290	0.37	0.0800	0.00640
3	0.2	0.677	0.66	-0.0167	0.00028
4	0.68	0.885	0.79	-0.0949	0.00900
5	0.68	0.885	0.78	-0.1049	0.01100
6	1.5	0.952	1.15	0.1984	0.03938
7	2.35	0.974	0.98	0.0034	0.00001
8	2.35	0.974	0.98	0.0034	0.00001
9	2.35	0.974	0.98	0.0104	0.00011
10	5.31	0.996	1.00	0.0038	0.00001
11	5.31	0.996	1.00	0.0038	0.00001
12	5.31	0.996	1.00	0.0038	0.00001
				Standard Error	0.0743
				Mean	0.0055
				Root Mean	0.0743
				RMS	**0.0062**

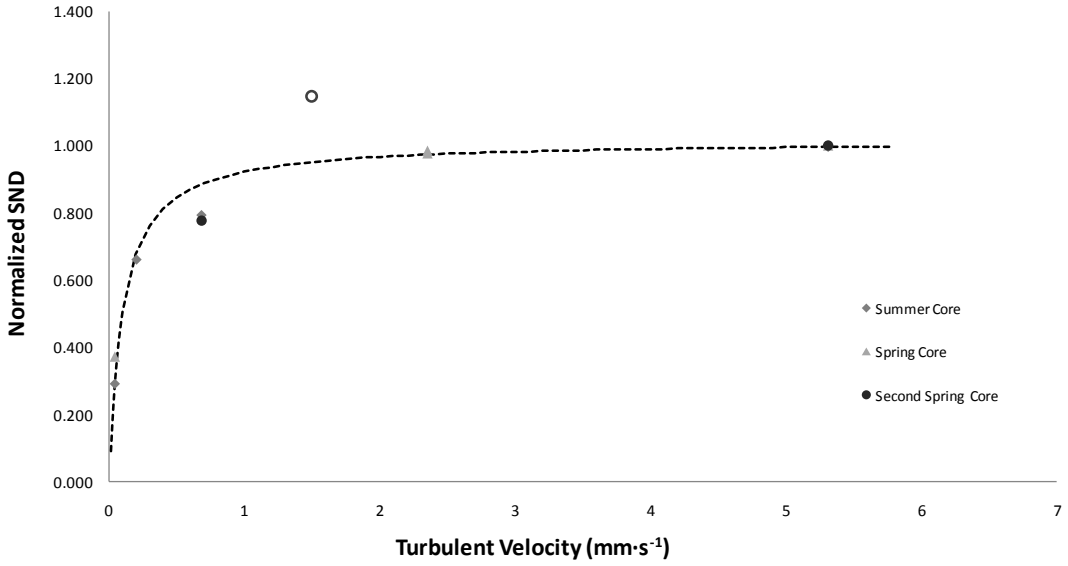

Figure 5.4: Normalized flux values from three separate sediment cores plotted against the vertical fluid velocity at the sediment water interface

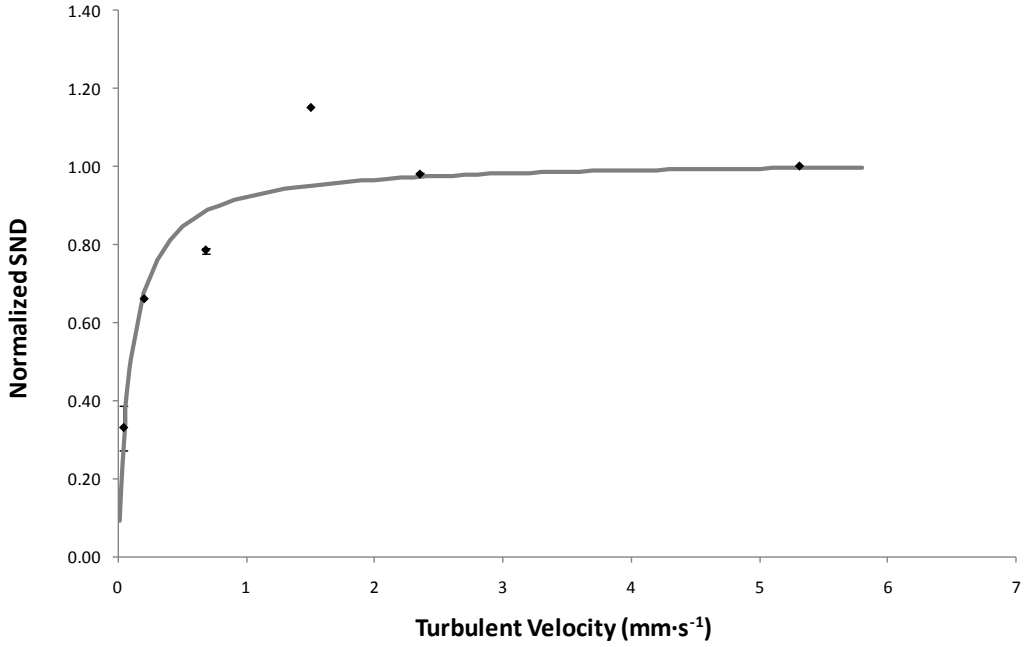

Figure 5.5: Averaged normal SND values from figure 6 plotted with error bars

5.4 Microprofiling Reactor Results

In the microprofiling experiment, flux values were measured for three different bulk liquid concentrations. Replicate profiles were taken at no less than 5 different mixing RPM settings at each bulk liquid condition until a curve could be selected that was representative of sediment characteristics (Figure 5.6).

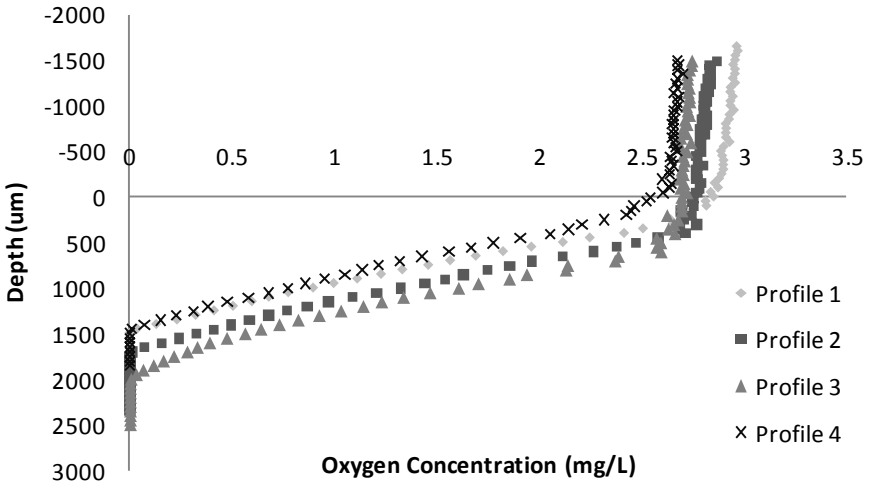

Figure 5.6: Sample of 4 profiles taken out of the core at a bulk liquid concentration of ~3 mgO2/L and a RPM setting of 12. Once it was determined that profiles all had similar comparable slopes, the slope was calculated and used to determine the flux at this condition using Ficks law (Section 4.5).

With multiple fluxes calculated, a curve was created to show the relationship flux and mixing RPM (Figure 5.7). This relationship was plotted for all three bulk liquid concentrations.

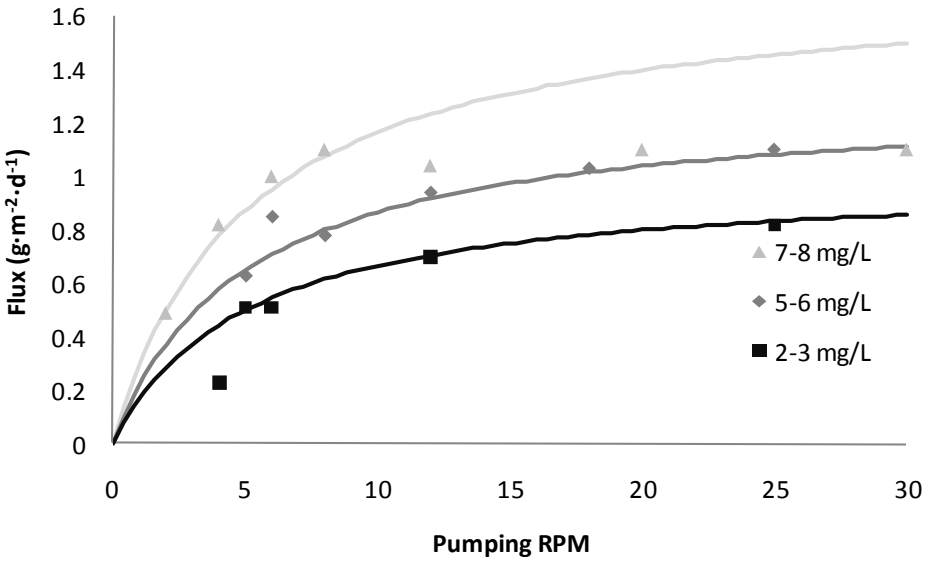

Figure 5.7: Sediment oxygen demand as measured by oxygen microprofiles at different turbulence levels and bulk liquid oxygen concentrations.

The SOD_{max} values obtained from the three different bulk liquid experiments ranged from 0.82 – 1.1 $gO_2 \cdot m^2 \cdot d^{-1}$. The max value occurred above a pumping mixing setting of 20 RPM. The SOD_{max} values compare favorably with the average SOD_{max} values obtained throgh the reactor experiment (1.09 $gO_2 \cdot m^{-2} \cdot day^{-1}$) and the AHOD values obtained for Onondaga Lake (1.02; UFI Unpublished).

Rectangular hyperbola were fit to each set of data using equation 5. The 7-8 $mgO_2 \cdot L^{-1}$ curve resulted in an α of 1.75 and a β of 5.0. The 5-6 $mgO_2 \cdot L^{-1}$ curve resulted in an α of 1.3 and a β of 5.0. Finally, the 2-3 $mgO_2 \cdot L^{-1}$ curve resulted in an α of 1.0 and a β of 5.0. The profile curve of 2-3 $mgO_2 \cdot L^{-1}$ in the bulk liquid results in the closes match to the curve found in the reactor experiment (α = 1.05 and β = 0.2). The curves from figure 5.7 all seem to fit the data points fairly well except for the curve in the 7-8 $mgO_2 \cdot L^{-1}$ curve. The last few points do not fit on the line decided to represent the data. It was concluded

that these three points were not profided enough time to reach steady state and as a result, the curve of best fit was fit to the lower 4 points on the curve.

5.5 Comparison of Flux Calcuation Methods

Two different flux calculation methods were used in this experiment to be confident in calculated results. The steady state reactor experiment was used as the main method and all final results are drawn from this method. The microprofiling method was used to verify that fluxes calculated from the core experiment were reliable. Data for a third method (the AHOD method) was borrowed from the Upstate Freshwater institute to further verify the results.

From the data above, fluxes calculated from each method compared favorably. The steady state reactor experiment resulted in an average flux of 1.09 ± 0.11 $gO_2 \cdot m^{-2} \cdot day^{-1}$. The profile experiment resulted in a flux range from 0.82 - 1.1 $gO_2 \cdot m^{-2} \cdot day^{-1}$. Finally the AHOD method resulted in a 1.02 $gO_2 \cdot m^{-2} \cdot day^{-1}$ average flux. The values obtained from these methods overlap, suggesting that the results from each method are not significantly different from one another. This also suggests that all 3 methods are a viable technique for determining SOD.

In comparing the steady state reactor method to the microprofiling method, the curves with similar bulk liquid concentrations should be compared. Curves from both experiments resulted in bulk liquid concentrations in the 2-3 $mgO_2 \cdot L^{-1}$. For this range, the microprofiling experiment resulted in a flux of 0.82 $gO_2 \cdot m^{-2} \cdot day^{-1}$. This is 25% lower than the average value obtained in the steady state core experiment. The difference can

be attributed to the variation of fluxes between cores and seasonal differences, as similar variations were also seen between cores in the steady state reactor experiment.

Unfortunately, a full comparison of the two methods cannot be made due to differences in the experiments. The original reactor created for the steady state flux experiment was not designed to accommodate microprofiling. As a result, a different core design had to be modified to use in the experimental set up described in figure 4.2. This new core was not analyzed with particle velocimetry and as a result, RPM values can't be converted into fluid velocities to complete a full comparison of the two methods. General observational comparisons can be made however. As can be seen in comparing figures 5.3 and 5.7, the rectangular hyperbola shape of the curve caused by the DBL exists in both methods of experimentation, further suggesting the existence of the DBL. The curve from the microprofiling experiment that most closely matches figure 5.3 by comparing the α and β values is the curve from 2-3 $mgO_2 \cdot L^{-1}$. This is encouraging since our steady state reactor experiments were run in this range, but again, no absolute conclusions can be drawn due to our inability to quantify turbulence in the microprofile experiment.

An important thing to note from the microprofile experiment is the change seen in SOD with increasing bulk liquid concentrations. This experiment showed that higher bulk liquid concentrations result in higher SOD values. It is because of this phenomenon that when measuring flux values using the steady state method, similar bulk liquid concentrations had to be achieved before a flux value was taken. Figure 5.7 can then be used to determine how large of an impact changing the bulk liquid concentration can have on the SOD. At high bulk liquid concentrations (ie, between curves 5-6 and 7-8 $mgO_2 \cdot L^{-1}$ in figure 5.7), it was calculated that for an increase in the bulk liquid oxygen

concentration of 1 $mgO_2 \cdot L^{-1}$, we would expect to see a 17% increase in SOD. At low bulk liquid concentrations (ie, between curves 2-3 and 5-6 $mgO_2 \cdot L^{-1}$ in figure 5.7), it was calculated that for an increase in the bulk liquid oxygen concentration of 1 $mgO_2 \cdot L^{-1}$, we would expect to see a 10% increase in SOD. This shows that at lower bulk liquid oxygen concentrations, we would expect that changes in the bulk liquid concentration would have less of an impact on the SOD as they do at higher bulk liquid concentrations. We can use this to determine the approximate variation in our final calculated fluxes for our oxygen reactor experiments. Our oxygen reactor experiments resulted in an average of 2.96 ± 1.86 $mgO_2 \cdot L^{-1}$. It can be assumed that the observed variation in bulk liquid oxygen concentrations would result in a final SOD variation of 18.6%. Assuming these percentages hold true for our nitrate reactor experiments, the variation in the final nitrate fluxes can also be calculated. The nitrate reactor experiments saw an average flux of 2.12 ± 0.76 $gN \cdot m^{-2} \cdot day^{-1}$. From this we can assume that the variation in the bulk liquid nitrate concentration would result in a 7.6% variation in our final SND values. However this relationship may not hold true for changes in the bulk liquid nitrate concentrations.

5.6 Turbulence and Induced SOD/SND in Onondaga Lake

As discussed above, the SND/SOD realized in a particular lake may be substantially less than the value for SND/SOD_{max} due to the presence of boundary layer (turbulence) effects. The relationships between turbulence and chemical flux presented here (Figures 5.2 and 5.4) demonstrate that this induced demand can be significant. For this reason, turbulence introduced to the hypolimnion during electron acceptor amendment must be accommodated (as an additional demand) in system design. The results presented here can support the design and implementation of such a system for Onondaga Lake.

An induced demand effect is clearly evident for velocities <~1.5 mm·s^{-1}, i.e. at and below the elbow in Figures 5.2 and 5.4. Departure of the observed SND/SOD from SND/SOD$_{max}$, is conservatively estimated to occur at 2.0 mm·s^{-1}. This same phenomenon is seen in the microprofiling experiment as well, although the exact departure velocity cannot be determined. If ambient hypolimnetic velocities are below this departure velocity (2.0 mm·s^{-1}; Figure 5.6), increases in turbulence would result in induced demand. Conversely, if the ambient velocity is greater than the departure velocity, little or no change in SOD/SND would be expected. Below a certain critical velocity, sediment demand decreases rapidly. Critical velocities were arbitrarily assigned as 90% of SOD/SND$_{max}$(Figure 5.6). Lakes with ambient turbulences existing below the critical velocity will experience elevated levels of induced demand if electron acceptor amendment systems are installed. Cowen and Rusello (2008) measured a mean hypolimnetic turbulence for Onondaga Lake of 1-1.5 mm·s^{-1} (October, stratified conditions) which is below the departure velocity of 2 mm·s^{-1} but matches or is above the critical velocity (Figure 5.6). Thus, increases in turbulence associated with electron acceptor augmentation would be expected to exhibit a modest induced SND/SOD (Figure 5.6).

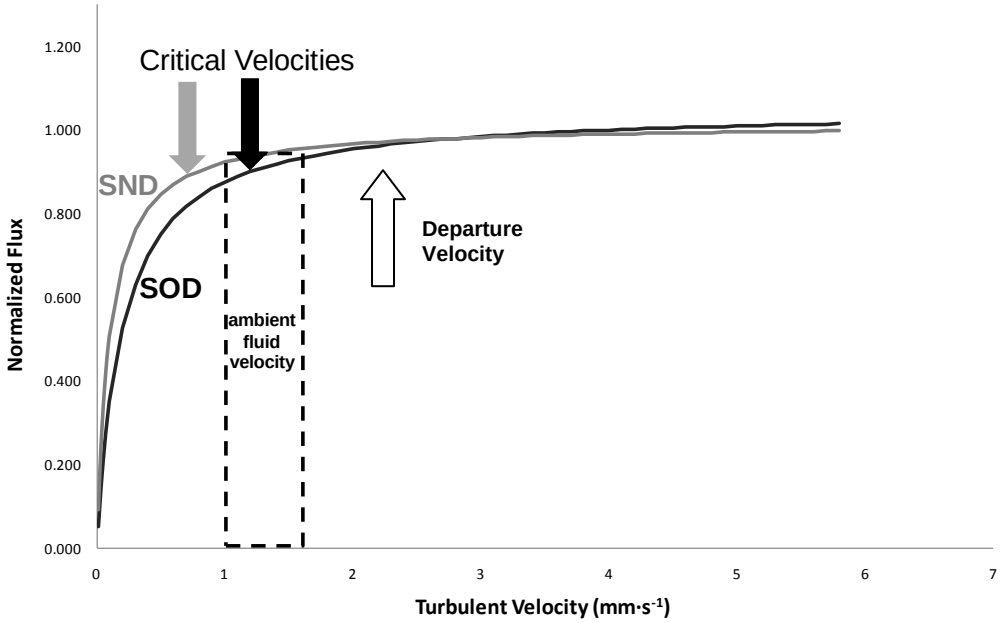

Figure 5.8: Natural turbulence at the sediment water interface plotted on the turbulence SOD/SND relationship figures. Critical velocities were arbitrarily determined and plotted as 90% of maximum flux.

Fluid velocities of 1-1.5 $mm \cdot s^{-1}$ put Onondaga Lake near the plateau of the induced demand curve (Figure 5.6). As a result, induced demand would only be expected to exhibit an increase of ~5-8% for SND and ~8-14% for SOD. Soltero et al. (1994) performed a study on Medical Lake in Washington and discovered a 2 fold increase in the SOD after oxygen diffuser implementation. Another study by Smith et al. (1975) discovered that on Larson Lake, post implementation oxygen demands could be 3-4 times greater than pre implementation values. This compares favorably with Figures 5.2 and 5.4. Three or four fold increases in SOD would be expected to occur at fluid velocities around .3 $mm \cdot s^{-1}$. This is slightly lower than the potential measurement range of this experiment. This suggests that Onondaga Lake is at the high end of the range for hypolimnetic fluid velocities and as a result, would see lesser effects from induced demand. This is consistent with its elongated morphometry making it susceptible to

sieche activity through wind mixing. Although the induced demand for Onondaga Lake is small, it should be accounted for in the design of an electron acceptor amendment system to prevent depletion. Ideally, this experiment could be performed on other lakes as well to aide in designing electron acceptor amendment systems through characterizing induced demand.

6.0 Conclusions

This research was successful in quantifying the relationship between hypolimnion turbulence and SOD/SND in Onondaga Lake. It was concluded that fluid velocity has a very strong impact on the uptake of electron acceptors in to the sediments. Above a fluid velocity of ~2 $mm \cdot s^{-1}$, the DBL has been thinned near its minimum thickness and further increases in fluid velocity will no longer exhibit an induced demand. Below this velocity, SOD/SND drops off in the shape of a rectangular hyperbola. Lake environments that lie below the departure velocity (2 $mm \cdot s^{-1}$) will need to take induced demand into account in the design and implementation of electron acceptor ammendment systems.

Other studies have reported large increases in SOD (3-4 fold) resulting from induced demand. Onondaga Lake however exhibits natural hypolimnion fluid velocities that exist near the plateau of the demand/turbulence. This is due to its orientation towards the prevailing wind and susceptibility to seiching. As a result, Onondaga Lake would only expect to see modest increases in SOD (5-7%) and SND (8-14%) resulting from the implementation of an electron acceptor ammendment system.

The predicted increases in SOD/SND can be implemented into the design of an electron acceptor ammendment system for Onondaga Lake. If implemented correctly, under design of the system can be avoided and money can be saved through system optimization. This will aide in a MNR plan to prevent mercury releases from the sediments while the lake naturally recovers through sedimentation and burial processes.

Future Work and Recommendations

Further work should be done to more accurately quantify the bend in the demand/fluid velocity relationship. Due to a lack of time, this study only measured 6 turbulence levels to quantify the curve. More points near the bend would more accurately quantify the curve and yield more accurate quantifications of induced demand.

More data also needs to be gathered at the extremely low fluid velocities. More replicate points at fluid velocities below .5 $mm \cdot s^{-1}$ would better quantify the low velocity portion of the curve. These points would give a better understanding of how lakes with low ambient turbulences would respond to induced demand.

Another study that could be done that could help shed light in this field would be to analyze different types of electron acceptor ammendment systems for how much extra turbulence they impart on the water. Using this to quantify post implementation turbulence levels would help greatly in selecting and designing electron acceptor ammendment sytems for different purposes.

More data needs to be collected on the microprofiling experiment. In this experiment, the microprofiling work only served as verification of the existance of a boundary layer the comparison of flux calculation methods. If a better system was designed where turbulence was quantified and the reactor could be in continuous operation while profiles were being taken, this whole experiment could be repeated using the profiling method. This would help bring full closure to the analysis of boundary layers.

One final suggestion for future work would be to compare Onondaga Lake with more case studies of induced demand. Since Onondaga Lake seems to have a very high natural ambient turbulence level, it would be interesting to see if other lakes with similar

properties and qualities exhibit similar hypolimnion fluid velocities. This could provide a better understanding of what types of lakes are more susceptibele to induced demand.

References

Apitz S. E., Davis, J. W., Finkelstein, K., Hohreiter, D. W., Hoke, R., et al. 2005. Assessing and Managing Contaminated Sediments: Part I, Developing an Effective Investigation and Risk Evaluation Strategy. Integrated Environmental Assessment and Management: 1(1): 2–8

Arega, F., Lee, J. H. W., 2005. Diffusional mass transfer at sediment–water interface of cylindrical sediment oxygen demand chamber. Journal of Environmental Engineering 131:755-766.

Ashley, K. I., 1983. Hypolimnetic aeration of a naturally eutrophic lake: physical and chemical effects. Canadian Journal of Fisheries and Aquatic Sciences 40 (9): 1343-1359.

Beutel, M. W., 2003. Hypolimnetic anoxia and sediment oxygen demand in California drinking water reservoirs. Lake Reservoir Management 19: 208–221

Beutel, M. W., 2006. Inhibition of ammonia release from anoxic profundal sediments in lakes using hypolimnetic oxygenation. Ecological Engineering 28 (3): 271-279.

Bloom, N. S., Effler, S. W., 1990. Seasonal variability in the mercury speciation of Onondaga Lake(New York). Water, Air, and Soil pollution 53 (3-4): 251-265.

Boynton, W. R., Kemp, W. M., Osborne, C. G., Kaymeyer K. R., Jenkins, M. C., 1981. Influence of water circulation rate on in-situ measurements of benthic community respiration. Marine Biology 65 (2): 185-190.

Cai, W. J., Sayles, F., 1996. Oxygen Penetration Depths and Fluxes in Marine Sediments. Marine Chemistry 52 (2): 123-131.

Canale, R. P., Effler, S. W., 1989. Stochastic Phosphorous Model for Onondaga Lake. Water Research 23 (8): 1009-1016.

Carpenter, J. H., Pritchard, D. W., Whaley, R. *C.,* 1969. Observations of eutrophication and nutrient cycles in some coastal plain estuaries. In: Eutrophication: causes. consequences, corrections. National Academy of Sciences. Washington, pp. 210-221

Cowen, E. A., Rusello, P. J., 2008. Memorandum on fall 2007 preliminary field observations of hypolimnetic turbulence levels in onondaga lake. Unpublished.

Correll, D. L. 1999. Phosphorus: a rate limiting nutrient in surface waters. Poultry Science 78 (5): 674-682.

Dales, L., Kahn, E., Wei, E., 1970. Methylmercury poisoning: An assessment of the sportfish hazard in California. California and Western Medicine. 114(3): 13–15.

Devan, S. P., Effler, S. W., 1984. History of phosphorus loading to Onondaga Lake. Journal of Environmental Engineering 110 (1): 93-109.

Driscoll, C. T., Yan, C., Schofield, C. L., Munson, R., Holsapple, J., 1994. The mercury cycle and fish in the Adirondack lakes. Environmental Science & Technology 28 (3): 136-143.

Erickson, M. J., Auer, M. T., 1998. Chemical exchange at the sediment water interface of Cannonsville Reservoior. Lake and Reservoir Management. 14(2-3):266-277

Effler, S. W. 1987. The impact of a chlor-alkali plant on Onondaga Lake and adjoining systems. Water, Air, and Soil Pollution 33 (1): 85-115.

Effler, S. W., Hassett, J. P., Auer, M. T., Johnson, N., 1988. Depletion of epilimnetic oxygen and accumulation of hydrogen sulfide in the hypolimnion of Onondaga Lake, NY, USA. Water, air, and soil pollution 39 (1): 59-74.

Effler,S. W., 1996. Limnological and Engineering Analysis of a Polluted Urban lake. 1 ed. Springer Series on Environmental Management. 1, Prelude to Environmental Management of Onondaga Lake, New York. Steven W. Effler. New York: Springer-Verlag.

Effler, S. W. O Donnell, S. M. Matthews, D. A. O Donnell, D. M., Auer, M. T., Owens, E. M., 2002. Limnological and Loading Information and a Phosphorus Total Maximum Daily Load (TMDL) Analysis for Onondaga Lake. Lake and Reservoir Management. 18 (2): 87-108

Feibicke, M.,1997. Impact of nitrate addition on phosphorus availability in sediment and water column and on plankton biomass—Experimental field study in the shallow brackish schlei Fjord (Western Baltic, Germany). Water, Air, and Soil Pollution 99 (1): 445-456.

Gagnon, C., Pelletier, E., Mucci, A., Fitzgerald, W. F., 1996. Diagenetic behavior of methylmercury in organic-rich coastal sediments. Limnology and Oceanography 41 (3): 428-434.

Galicinao, G. A. E., 2009. Determination of methylmercury flux from Onondaga Lake sediments using flow-through reactors. M.S. Thesis, Department of Civil & Environmental Engineering, Michigan Technological University, Houghton, MI, 91 pp.

Gantzer, P. A., Bryant, L. D., Little, J. C., 2009. Effect of hypolimnetic oxygenation on oxygen depletion rates in two water-supply reservoirs. Water Research 43 (6): 1700-1710.

Gbondo-Tugbawa, S., Driscoll, C. T., 1998. Application of the regional mercury cycling model (RMCM) to predict the fate and remediation of mercury in Onondaga Lake, New York. Water, Air, and Soil Pollution 105 (1): 417-426.

Gelda, R. K., Auer, M. T., and Effler, S. W., 1995. Determination of sediment oxygen demand by direct measurement and by inference from reduced species accumulation. Marine and Freshwater Research 46, 81–88.

Gemza, A. F., 1997. Water quality improvements during hypolimnetic oxygenation in two Ontario lakes. Water Quality Research Journal of Canada. 365-390

Graetz, D. A., Keeney, D. R., Aspiras, R. B., 1973. Eh status of lake sediment-water systems in relation to nitrogen transformations. Limnology and Oceanography 18 (6): 908-917.

Gundersen, J. K., Jorgensen, B. B. (1990). Microstructure of diffusive boundary layers and the oxygen uptake of the sea floor. Nature, Lond. 345: 604-607

Hall, P. O. J., Anderson, L. G., Rutgers van der Loeff, M. M., Sundby B., and Westerlund, S. F. G., 1989. Oxygen uptake kinetics in the benthic boundary layer. Limnology and Oceanography 34 (4): 734-746.

Hansen, J., Reitzel, K., Jensen, H. S., Andersen, F. Ø., 2003. Effects of aluminum, iron, oxygen and nitrate additions on phosphorus release from the sediment of a Danish softwater lake. Hydrobiologia 492 (1): 139-149.

Hines, M. E., Horvat, M., Faganeli, J., Bonzongo, J. C. J., Barkay, T., Major, E. B., Scott, K. J., Bailey, E. A., Warwick, J. J., Lyons, W. B., 2000. Mercury biogeochemistry in the Idrija River, Slovenia, from above the mine into the Gulf of Trieste. Environmental Research 83 (2): 129-139.

Jensen, S. Jernelov, A. 1969. Biological methylation of mercury in aquatic organisms. Nature 223, 753 - 754

Jorgensen, B. B., Des Marais, D. J. (1990). The diffusive boundary layer of sediments: oxygen microgradients over a microbial mat. Limnology and Oceanography 35: 1343-1355

Jorgensen, B. B., Revsbech, N. P., 1985. Diffusive boundary layers and the oxygen uptake of sediments and detritus. Limnology and Oceanography 30 (1): 111-122.

Lambertsson, L., Nilsson, M., 2006. Organic material: the primary control on mercury methylation and ambient methyl mercury concentrations in estuarine sediments. Environmental Science & Technology 40 (6): 1822-1829.

Manohar, D. M. Krishnan, K. A., Anirudhan, T. S., 2002. Removal of mercury (II) from aqueous solutions and chlor-alkali industry wastewater using 2-mercaptobenzimidazole-clay. Water Research 36 (6): 1609-1619.

Matthews, D. A., Effler, S. W., 2006. Long-term changes in the areal hypolimnetic oxygen deficit(AHOD) of Onondaga Lake: Evidence of sediment feedback. Limnology and oceanography 51 (1): 702-714.

Matthews, D. A., Effler, S. W., Driscoll, C. T., Odonnell, C. T., Matthews, C. M., 2008. Electron budgets for the hypolimnion of a recovering urban lake, 1989- 2004: Response to changes in organic carbon deposition and availability of electron acceptors. Limnology and Oceanography 53 (2): 743-759.

McQueen, D. J., Lean, D. R. S. 1986. Hypolimnetic aeration: An overview. Water quality Research Journal of Canada 21 (2): 205-217.

McDonnell, A. J., Hall, S. D. 1969. Effect of environmental factors on benthal oxygen uptake. Journal - Water Pollution Control Federation 41 (8): 353-363.

Moore, B. C. 1996. A model for predicting lake sediment oxygen demand following hypolimnetic aeration. Journal of the American Water Resources Association 32 (4): 723-731.

New York State Department of Environmental Conservation (NYSDEC). 2005. Record of Decision: Onondaga Lake bottom subsite of the Onondaga Lake superfund site, Towns of Geddes and Salina, Villages of Solvay and Liverpool, and City of Syracuse, Onondaga County, New York. New York.
State Department of Environmental Conservation, Albany, NY.

Niirnberg, G. K., 1984. The prediction of internal phosphorus load in lakes with anoxic hypolimnia. Limnology and Oceanography 29 : 111-124.

Oremland, R. S., Miller, L. G., Dowdle, P., Connell, T., Barkay, T., 1995. Methylmercury oxidative degradation potentials in contaminated and pristine sediments of the Carson River, Nevada. Applied and Environmental Microbiology 61 (7): 2745-2753.

Pak, K. R., Bartha, R., 1998. Mercury methylation and demethylation in anoxic lake sediments and by strictly anaerobic bacteria. Applied and Environmental Microbiology 64 (3): 1013-1017.

Parks, J. W., Lutz, A., Sutton, J. A., 1989. Water column methylmercury in the Wabigoon/English River-Lake system: Factors controlling concentrations, speciation, and net production. Canadian Journal of Fisheries and Aquatic Sciences 46 (12): 2184-2202.

Reimers, R. S., Krenkel, P. A., 1974. Kinetics of mercury adsorption and desorption in sediments. Journal - Water Pollution Control Federation : 352-365.

Rusello, P.J. and Cowen, E.A. 2010. A turbulent microcosm chamber for laboratory scalar flux estimates. In preparation for *Water Resources Research*

Ripl, W., 1976. Biochemical oxidation of polluted lake sediment with nitrate: a new lake restoration method. Ambio : 132-135.

Smith, S. A., D. R. Knauer, and T. L. Wirth. 1975. *Aeration as a lake management technique.* Technical Bulletin No. 87, Wisconsin Department of Natural Resources, Box 450, Madison 53701, 40 p.

Soltero, R. A., Sexton, L. M., Ashley, K. I., McKee, K. O., 1994. Partial and full lift hypolimnetic aeration of Medical Lake, WA to improve water quality. Water Research 28 (11): 2297-2308.

Sundby, B. 1986. The effect of oxygen on release and uptake of cobalt, manganese, iron and phosphate at the sediment-water interface. Geochimica et Cosmochimica Acta 50 : 1281-1288.

Swain, E. B. 1992. Increasing rates of atmospheric mercury deposition in midcontinental North America. Science 257 (5071): 784-787.

Taggart, C. T., McQueen, D. J., 1982. A model for the design of hypolimnetic aerators. Water Research 16(6): 949-956.

Ullrich, S. M., Tanton, T. W., Abdrashitova, S. A., 2001. Mercury in the aquatic environment: a review of factors affecting methylation. Critical Reviews in Environmental Science and Technology 31 (3): 241-293.

Watras, C. J., Back, R. C., Halvorsen, S., Hudson, R. J. M., Morrison, K. A., Wente, S. P., 1998. Bioaccumulation of mercury in pelagic freshwater food webs. The Science of the Total Environment 219 (2-3): 183-208.

Winfrey, M. R., Rudd, J. W. M., 1990. Environmental factors affecting the formation of methylmercury in low PH lakes. Environmental Toxicology and Chemistry: Vol. 9, No. 7 pp. 853–869

Wodka, M. C., Effler, S. W., Driscoll, C. T., Field, S. D., and Devan, S. P., 1983. Diffusivity-based flux of phosphorus in Onondaga Lake. Journal of Environmental Engineering 109 (6): 1403-1415.

Wodka, M. C., Effler, S. W., Driscoll, C. T., 1985. Phosphorus deposition from the epilimnion of Onondaga Lake. Limnology and Oceanography : 833-843.

Zeller, C., Cushing, B., 2006. Panel discussion: remedy effectiveness: what works, what doesn. Integrated Environmental Assessment and Management 2 (1): 75-79.

Table A. 1. Composition of Artificial Lake Water, according to the ionic composition of Onondaga Lake for sediment microcosm applications

Salt	Final Concentration (mM)	Final Concentration ($mg \cdot L^{-1}$)
CaCl2.2H2O	5.84	858.83
NaHCO3	4.24	356.2
(Na)2SO4	1.67	237.21
MgCl2.6H2O	0.99	200.87
KCl	0.44	32.43
NaCl	3.21	187.45
NaF	0.02	1.01

Cations	($meq \cdot L^{-1}$)	(mM)	(mg/L)
Ca	40.08	5.842	234.14
K	39.0983	0.435	17.01
Mg	24.305	0.988	24.03
Na	22.9898	10.812	248.57
Total	**24.908**		

Anions	($meq \cdot L^{-1}$)	(mM)	(mg/L)
Cl-	17.303	17.303	611.54
HCO3-	4.241	4.241	258.64
F	0.024	0.024	160.42
SO4-	3.340	1.670	0.46
Total	**24.908**		

Table A. 2. Summary of results all oxygen reactor incubations

Summer Cores (Installed 8/8/08, SNDmax = 1.07 g $O_2 \cdot m^{-2} \cdot d^{-1}$)							
Start Date	Pump RPM	Pump Velocity ($mm \cdot s^{-1}$)	C_{ss} ($mg\ O_2 \cdot L^{-1}$)	flux ($g\ O_2 \cdot m^{-2} \cdot d^{-1}$)	Standard Deviation	Normalized Flux	Results Accepted?
8/8/2008	6	0.2	6.4	0.79	0.01	0.74	Yes
8/5/2008	6	0.2	3.1	0.84	0.02	0.79	Yes
8/13/2008	25	1.8	6.0	1.01	0.02	0.95	Yes
8/19/2008	25	1.8	5.6	1.07	0.01	1.00	Yes
11/7/2008	2	0.04	1.9	0.50	0.02	0.47	Yes

Late Summer/Fall Core (Installed 10/7/08, SNDmax = 1.25 g $O_2 \cdot m^{-2} \cdot d^{-1}$)							
Start Date	Pump RPM	Pump Velocity ($mm \cdot s^{-1}$)	C_{ss} ($mg\ O_2 \cdot L^{-1}$)	flux ($g\ O_2 \cdot m^{-2} \cdot d^{-1}$)	Standard Deviation	Normalized Flux	Results Accepted?
10/7/2008	25	1.8	0.7	1.25	0.01	1.00	Yes
1/17/2009	10	0.5	1.6	0.80	0.01	0.64	Yes
1/23/2009	10	0.5	4.3	0.57	0.05	0.46	No, organic Carbon consumed in core
2/11/2009	50	4.3	4.2	0.56	0.05	0.45	No, core lost due to cold room failure

Spring Core 1 (Installed 4/14/09, SNDmax = 1.01 g $O_2 \cdot m^{-2} \cdot d^{-1}$)							
Start Date	Pump RPM	Pump Velocity ($mm \cdot s^{-1}$)	C_{ss} ($mg\ O_2 \cdot L^{-1}$)	flux ($g\ O_2 \cdot m^{-2} \cdot d^{-1}$)	Standard Deviation	Normalized Flux	Results Accepted?
4/14/2009	10	0.5	5.6	0.47	0.00	0.47	No, fresh core from 4 Degree C lake hypolimnion
5/3/2009	25	1.8	4.9	0.63	0.02	0.62	No, core still acclimating to 8 degree conditions
5/16/2009	10	0.5	3.4	0.73	0.00	0.72	Yes
6/12/2009	50	4.3	3.8	1.01	0.02	1.00	Yes
6/21/2009	25	1.8	1.9	1.37	0.03	1.36	Yes
7/1/2009	50	4.3	1.2	1.01	0.01	1.00	Yes
7/13/2009	17.5	1.2	1.8	0.65	0.00	0.64	No, organic carbon burnt up. Core is 3 months old

Spring Core 2 (Installed 7/28/09, SNDmax = 1.03 g $O_2 \cdot m^{-2} \cdot d^{-1}$)							
Start Date	Pump RPM	Pump Velocity ($mm \cdot s^{-1}$)	C_{ss} ($mg\ O_2 \cdot L^{-1}$)	flux ($g\ O_2 \cdot m^{-2} \cdot d^{-1}$)	Standard Deviation	Normalized Flux	Results Accepted?
7/28/2009	50	4.3	2.6	1.29	0.02	1.26	Yes
8/19/2009	17.5	1.2	2.0	0.97	0.02	0.94	Yes
8/29/2009	10	0.5	1.864	0.628	0.007	0.61	Yes
9/3/2009	50	4.3	1.89	1.03	0.002	1.00	Yes

Table A. 3. Summary of all results from nitrate reactor incubations

Summer Core (Installed 6/12/08, SNDmax = .079 $g \cdot m^{-2} \cdot d^{-1}$)							
Start Date	**Pump RPM**	**Pump Velocity ($mm \cdot s^{-1}$)**	**C_{ss} ($mg\ N \cdot L^{-1}$)**	**flux ($g\ N \cdot m^{-2} \cdot d^{-1}$)**	**Standard Deviation**	**Normalized Flux**	**Results Accepted?**
6/12/2008	**10**	0.5	1.56	0.063	0.006	0.793	Yes
6/15/2008	**50**	4.3	0.404	0.079	0.006	0.996	Yes
6/24/2008	**2**	0.04	2.73	0.023	0.008	0.290	Yes
7/17/2008	**6**	0.2	1.38	0.052	0.004	0.660	Yes
Late Summer/Fall Core (Installed 10/16/08, SNDmax = .18 $g \cdot m^{-2} \cdot d^{-1}$)							
Start Date	**Pump RPM**	**Pump Velocity ($mm \cdot s^{-1}$)**	**C_{ss} ($mg\ N \cdot L^{-1}$)**	**flux ($g\ N \cdot m^{-2} \cdot d^{-1}$)**	**Standard Deviation**	**Normalized Flux**	**Results Accepted?**
10/16/2008	**25**	1.8	3.61	0.18	0.03	0.977	Yes, but no points to compare against
Spring Core 1 (Installed 4/28/09, SNDmax = .258 $g \cdot m^{-2} \cdot d^{-1}$)							
Start Date	**Pump RPM**	**Pump Velocity ($mm \cdot s^{-1}$)**	**C_{ss} ($mg\ N \cdot L^{-1}$)**	**flux ($g\ N \cdot m^{-2} \cdot d^{-1}$)**	**Standard Deviation**	**Normalized Flux**	**Results Accepted?**
4/28/2009	**10**	0.5	2.37	0.285	0.033		No, First experiment with fresh core from storage
5/3/2009	**25**	1.8	2.56	0.252	0.030	0.977	Yes
6/7/2009	**2**	0.04	2.73	0.096	0.022	0.372	Yes
6/15/2009	**50**	4.3	2.96	0.258	0.036	1.000	Yes
6/23/2009	**25**	1.8	2.51	0.254	0.028	0.984	Yes
7/14/2009	**17.5**	1.2	2.209	0.086	0.008	0.333	No, core is exhausted of organic carbon
Spring Core 2 (Installed 7/29/09, SNDmax = .158 $g \cdot m^{-2} \cdot d^{-1}$)							
Start Date	**Pump RPM**	**Pump Velocity ($mm \cdot s^{-1}$)**	**C_{ss} ($mg\ N \cdot L^{-1}$)**	**flux ($g\ N \cdot m^{-2} \cdot d^{-1}$)**	**Standard Deviation**	**Normalized Flux**	**Results Accepted?**
7/29/2009	**50**	4.3	2.68	0.289	0.016	1.829	No, First experiment with fresh core from storage
8/20/2009	**17.5**	1.2	2.23	0.181	0.01	1.146	Yes
8/28/2009	**10**	0.5	1.88	0.123	0.004	0.778	Yes
9/4/2009	**50**	4.3	2.39	0.158	0.006	1.000	Yes

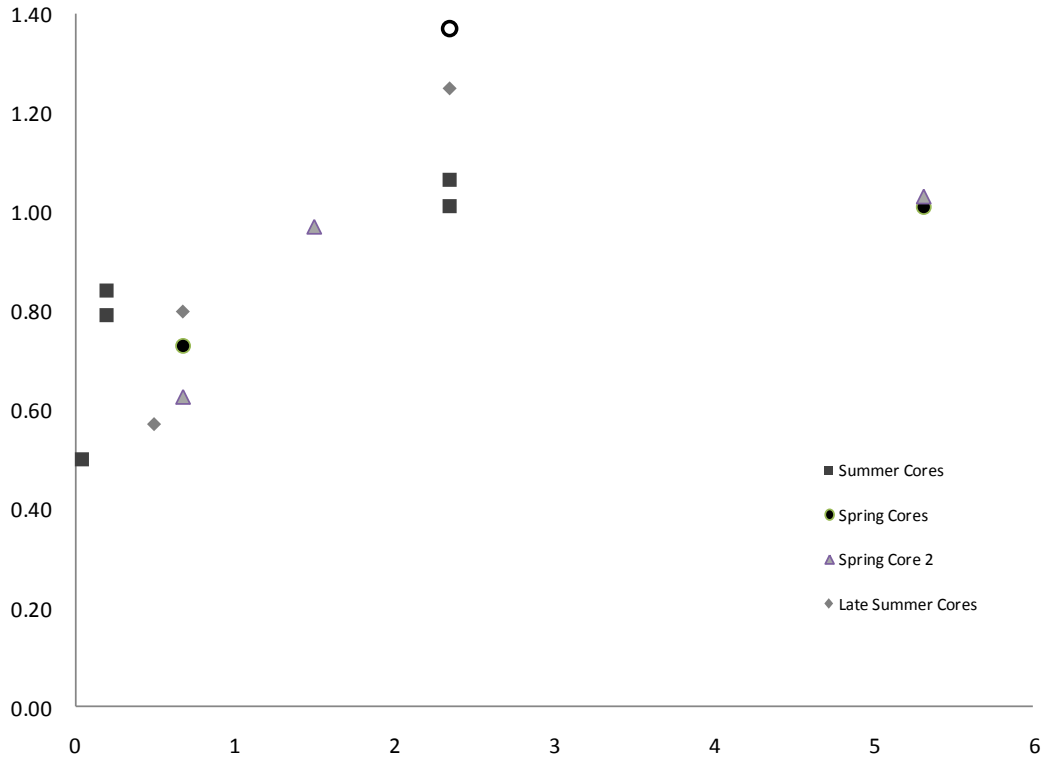

Figure A. 1. Non normalized results gathered from the steady state oxygen experiment.

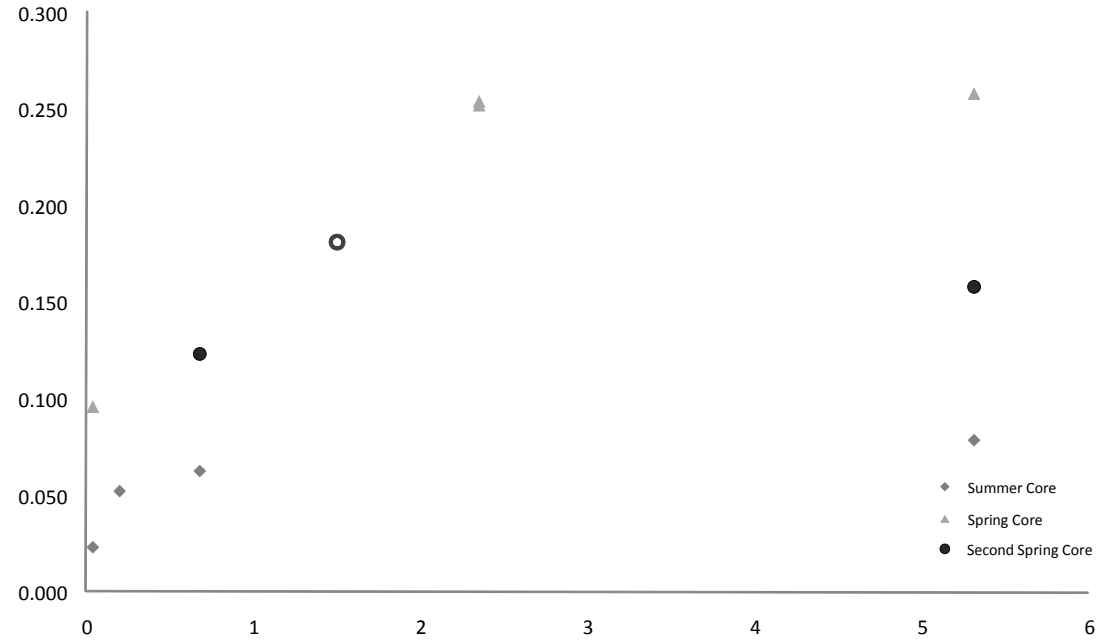

Figure A. 2. Non normalized results gathered from the steady state nitrate experiment.

Appendix B

Methods for Bromide Diffusion Experiment

Experiment Set-up

1. Create a stock solution of 100mg/L Br- by adding 148.94 mg KBr to 1 liter of DI water.
2. Remove the water from above the sediment core (supernatant) with a syringe, taking care not to disturb the sediment.
3. Replace the supernatant water with 100 mL of the 100 mg/L Br- stock solution. Take Care when adding so as not to disturb the sediment.
4. Repeat 2-3 as necessary for each core.
5. Store cores upright at 8 degrees until harvest.

Harvest

1. Harvest Cores at 0, 0.5, 2, 6, 12, and 19 days.
2. Using a syringe, draw a sample of the supernatant and filter into an IC vial for analysis of Br- concentration.
3. Carefully remove the remaining supernatant.
4. Using the core slicing apparatus, slice core into 0.5cm slices, placing each sediment slice into its own centrifuge tube.
5. Once the core is completely sliced, centrifuge the samples until the pore water is separated from the sediment (~2000 RPM, 20 min, room temp.)
6. Pour the water into a vacuum filtration apparatus and filter though a glass microfiber filter to remove suspended particles.
7. Pour the filtrate into a graduated cylinder and record the volume. Empty into an IC vial.
8. Measure as many mL of DI water as needed to bring the total sample volume to ~7 mL. Record the volume added.
9. Insert the filter cap into the IC vial so it just starts to seal, then mix the sample by inverting the vial ~5 times. Insert the filter cap further until the top of the cap is level with the top of the vial (some liquid may come out of the filter cap, but since the sample is already mixed, the lost liquid is not of concern)
10. Analyze samples using Ion Chromatography

Ion Chromatography (IC)

1. Used 44mM NaOH eluent; Anion column (AS-16 column, I think)
2. Calibration curve generated using standards at concentrations of 1, 5, 10, 25, 50, and 100 mg/L Br-.
3. Full sets of standards were run at the beginning and end of each batch and partial sets were run between every 5-7 experimental samples. Vials of DI

water (blanks) were run between sets of standards and the experimental samples.

4. Using the calibration curve and results from the IC and the dilution of each sample at harvest time, the pore water Br- concentration can be calculated.